Istanbul Technical University

Bachelor's Thesis

Thermalization of Single-Mode Cavities

Supervisors:

Author:
Ceren Burçak Dağ

Prof. Özgür Müstecaplıoğlu
Koç University

Assoc. Prof. Ahmet Levent Subaşı
Istanbul Technical University

A thesis submitted in fulfilment of the requirements
for the Bachelors degree

in the

Physics Department
Faculty of Science and Letters

June 2015

Contents

Chapter 1

Introduction

Thermal interaction between two macroscopic systems requires an energy exchange between them, so that a non-equilibrium state reaches a thermal equilibrium with maximizing the total entropy, [1, 2]. Quantum thermal interaction, however, can exist between quantized microscopic systems such as atoms and particles. Like in classical thermal interaction, both thermalization and cooling can be observed for microscopic quantum systems. In fact understanding thermalization and cooling of a quantum system might be really fruitful in various areas of quantum information science from quantum heat engines [3, 4] and refrigerators [5, 6] all the way up to the design and construction of quantum computers [7, 8] and even biological quantum systems, [9, 10].

Quantum thermal interaction seems to be an intuitive phenomenon with energy and temperature equilibrium among the interacting systems, although only useful definition for the temperature of an atom requires that the atom should be in thermal state and has an energy structure of two-levels, [4] or in thermal state and has an energy structure of three-level with a level degeneracy, [11]. In this study, we are going to show that it is also possible to calculate the temperature of a thermal state system with three atoms when the state is symmetric. An ambiguity about quantum thermal interaction arises when atoms are chosen coherent rather than thermal. The coherency of the atoms is shown to be quite effective in the thermalization and hence the work capability of a quantum system, such as a cavity, [3, 11–14]. In fact, when a coherent atom is used, the temperature of the cavity exceeds the temperature of the thermal atom, which leads to a misconception of that coherently heated cavity's energy surpasses the energy of atom, which is totally counter-intuitive for thermal interaction. However, the coherency in the atom is not taken into account in this argument. It has been shown that the cost of adding coherency to a thermal reservoir is always greater than the work output of a photo-Carnot heat engine [15], which is an observation that quantum version of

heat engines does not violate any fundamental law of physics. A similar argument should be used for quantum thermal interaction, which intuitively requires an energy and temperature equilibrium between quantized systems, e.g. atomic reservoir and cavity for micromaser model, [16]. Although this ambiguity can be comprehended and justified, our research discusses another peculiar characteristic of quantum thermal interaction between an atomic reservoir with random injections and cavity in micromaser model. We report that some specific states can drive the cavity to lasing instead of thermalization, reminding that lasing with population inversion [17, 18] and lasing without population inversion (LWI) [16, 19] are expected behaviours of micromaser theory. However, the possibility of lasing instead of reaching a thermal equilibrium is counter-intuitive in the context of quantum thermal interaction, even though the explanation we presented in the text is reasonable.

For the investigation of quantum thermal interactions, Liao et al. [12] showed that the temperature information can be transferred from thermal atoms to the cavity, which is in fact the thermalization of atoms and cavity. Afterwards, Ref. [11] extended the analysis to 2-atom reservoirs and explicitly showed that specific coherence terms in a coherent reservoir can boost up the temperature of the cavity after thermalization is established. They also point out that quantum coherence is more important than quantum correlations in the extraction of work via radiation pressure in the cavity. In this study, we advance the calculations to 3-atom reservoirs and propose some practical rules for optimum thermalization with using the observations up to date. First of all, 3-atom reservoirs give us an opportunity to observe the effects of well-known entangled states, e.g. W and GHZ states [20]. W and GHZ states are distinctly different entangled states [21]. We are going to show that their distinct behaviours also pop up in a quantum thermal interaction. Finally we are going to draw conclusions regarding how thermalization can be re-established after the contact of a quantum reservoir and cavity as well as how optimum the thermalization can be with 3-atom reservoirs via a detailed examination of various states.

Increasing the number of atoms comes with its own difficulties, since basically the higher the numbers of atoms the wider the Hilbert space. Therefore, computation of evolution operators gets more involved and rigorous in a way that the modern classical computers cannot handle. However, the method we present in Appendix sort of bypasses aforementioned difficulties at least up to certain size of the Hilbert space. This method utilizes the transformation of spin product states into spin sum states in order to divide a complicated problem into little parts, [22]. Generalization of this method to N atoms might have utmost importance and utility for an analytical calculation of more rigorous systems under a quantum interaction, e.g. the Tavis-Cummings Model. Even though we presented the derivation of exact form of evolution operator, an approximated version

will suffice. Because we assume that the atoms pass through the cavity fast enough to apply instantaneous limit, $gt \to 0$. A general discussion of Jaynes-Cummings and Tavis-Cummings Models as well as the calculation of the evolution operators can be found in Chapter 3.

It is interesting to note that gain and loss channels for a non-dissipative cavity are defined via atomic reservoirs for thermalization models. This approach to the cavity loss takes a specific form at the level of master equation, which is coined as Lindblad form of master equation. To provide a comfortable introduction to master equations used in research, we give a general discussion on quantum loss and noise as well as Lindblad master equation in Chapter 2.

In Chapter 4, we are going to discuss essential concepts of quantum thermodynamics starting from quantum processes appearing in quantum heat engines (QHE). We are going to show that the existence of QHEs is important motivation to study quantum thermal interaction. Additionally, we are going to review most of the material in the literature on quantum thermal interactions.

Finally, in Chapter 6 we are going to summary our novel results.

Chapter 2

Lindblad Quantum Master Equation

We are going to give a brief introduction to modelling loss in quantum mechanics mostly conceptually, discuss the stochastic processes classically and introduce Lindblad quantum master equation, which is used throughout this thesis research.

2.1 Loss in quantum mechanics

Quantum mechanics quantifies the limit in the information we could have about a quantum mechanical system. In a way it quantifies the incompleteness of our information. Both Born's probability interpretation and Heisenberg's uncertainty principle are manifestations of this fundamental characteristics of quantum mechanics. This intrinsic statistical characteristic of quantum mechanics is one of the building blocks of quantum mechanical loss or quantum noise. However there is another significant aspect of quantum mechanical loss, which eventually reveals itself in every measurement process, which is the atomic decay.

Atomic decay is a phenomenon involving system-environment coupling. Since environment can consist of infinitely many electromagnetic modes in an electromagnetic field, an information-bearing system, e.g. an atom, will eventually interact with one of the modes existing in the environment. Such an exchange of energy is a manifestation of atomic decay and it gives rise to spectral lines of emission (and absorption). However, what is more interesting is that the atom will also slightly couple to neighbouring modes of resonance mode, as well. Therefore, the spectral lines will not be sharp, giving rise

to another mechanism of quantum mechanical loss, which actually originates from our inability to differentiate infinitely many modes in an electromagnetic field.

If there is a correlation between position and momentum operators, Heisenberg's uncertainty principle takes a more general form of,

$$\Delta x \Delta p \geq \sqrt{\hbar^2/4 + \sigma_{xp}^2}. \tag{2.1.1}$$

Here, σ_{xp}^2 is covariance with a mathematical condition of,

$$\left\langle \delta x^2 \right\rangle \left\langle \delta p^2 \right\rangle \geq \sigma_{xp}^2, \tag{2.1.2}$$

where $\left\langle \delta x^2 \right\rangle$ and $\left\langle \delta p^2 \right\rangle$ are variances for position and momentum operators, respectively. This is also the classical covariance, which is a measure of correlation between two variables in statistical theory, [23]. This covariance term has in fact an origin in the coupling of a system to a heat bath, which is one of the quantum loss mechanisms. Even though it has been classically derived, when the reservoir has quantum mechanical properties, this term can show quantum effects. So, it is not a purely classical term, although the term $\hbar^2/4$ in Eq. 2.1.1 is purely quantum mechanical, since the existence of this term totally depends on the commutation of x and p operators. Derivation of Eq. (2.1.1) can be found in Ref. [24].

2.1.1 Density matrices instead of wave functions

When loss is a factor in a quantum mechanical system, we cannot talk about closed systems any more. Because in an open system energy can be transferred to a heat bath or reservoir, so information of the system under study can simply get lost. However, we can model a problem in an open system as a problem in a closed system, so that our new closed system contains both the system and the reservoir. Then the interaction which lets the flow of energy from the system into reservoir can also be modelled. In fact due to this interaction, the problem is a time-dependent problem. Because of the reasons explained shortly, instead of using state vectors or wave functions $|\psi(t)\rangle$, we start to use density operator:

$$\rho(t) = |\psi(t)\rangle \langle\psi(t)| . \tag{2.1.3}$$

A density operator contains all the information that be found in a wave function. Additionally, it is a more general formulation than the state vector, because one can write down a density matrix for a statistical ensemble of states, namely a mixed state. On the other hand, a wave function can only be written for pure states. Let us a give an example. W state will be a topic in Chapter 5 in this thesis. So let us write down the

W state for three atoms,

$$|W\rangle = \frac{1}{\sqrt{3}} \left(|100\rangle + |010\rangle + |001\rangle \right). \tag{2.1.4}$$

So if we want to calculate the density matrix of W state, we would write,

$$\begin{aligned} \rho_W = \frac{1}{3} \left(|100\rangle \langle 100| + |010\rangle \langle 010| + |001\rangle \langle 001| + |100\rangle \langle 010| + |100\rangle \langle 001| \right) \\ + \frac{1}{3} \left(|010\rangle \langle 100| + |010\rangle \langle 001| + |001\rangle \langle 100| + |001\rangle \langle 101| \right). \end{aligned} \tag{2.1.5}$$

W state is a pure state, as can be seen in a state vector form, Eq. (2.1.4). What if we want to write Eq. (2.1.5) without its coherence terms, such as,

$$\rho_a = \frac{1}{3} \left(|100\rangle \langle 100| + |010\rangle \langle 010| + |001\rangle \langle 001| \right). \tag{2.1.6}$$

We cannot write Eq. (2.1.6) in a state vector form, but as seen it can be written in density matrix form because it's a mixed state. In short, density matrix formalism is indeed important for the study of open quantum systems. One should note that density matrices are the only way to write thermal states of light.

We can derive the equation of motion for the density operator from Schrödinger equation, too.

$$H |\psi(t)\rangle = i\hbar \frac{d}{dt} |\psi(t)\rangle \rightarrow \dot{\rho}(t) = \frac{-i}{\hbar} [H, \rho(t)]. \tag{2.1.7}$$

This equation is called Von Neumann's equation. Solving this equation, one can obtain the propagator of the system,

$$\rho(t) = \exp\left(\frac{-i}{\hbar} Ht \right) \rho(0) \exp\left(\frac{i}{\hbar} Ht \right), \tag{2.1.8}$$

where the propagator is $U(t) = \exp(-iHt/\hbar)$. The expected value of an operator is defined via,

$$\langle n(t) \rangle = \langle \psi(t)| n |\psi(t)\rangle = \mathrm{Tr}\left\{ n\rho(t) \right\}, \tag{2.1.9}$$

for the photon number operator n. The equation of motion for the operator n is then,

$$\dot{n}(t) = \frac{i}{\hbar} [H, n(t)]. \tag{2.1.10}$$

There are some important properties of density operators:

1. Normalizability of state vectors comes into picture as trace being equal to one.

$$\mathrm{Tr}\left\{ \rho \right\} = \sum_i P_i |\psi_i\rangle \langle \psi_i| = \sum_i P_i = 1. \tag{2.1.11}$$

2. ρ is positive semidefinite. For a state $|A\rangle$,

$$\langle A\,|\,\rho\,|\,A\rangle = \sum_i P_i |\,\langle A\,|\,\psi_i\rangle\,|^2 \geq 0. \tag{2.1.12}$$

3. For pure states,

$$\mathrm{Tr}\left\{\rho^2\right\} = 1. \tag{2.1.13}$$

If an ensemble of $|\psi\rangle$ has only one member, then that is a pure state since the system is always in the state $|\psi\rangle$. For mixed states, it can be shown that

$$\mathrm{Tr}\left\{\rho^2\right\} < 1. \tag{2.1.14}$$

Therefore by the last property, one can definitely differentiate pure and mixed states. Proofs of the properties and more detailed information regarding the mathematics of this section can be found via different quantum information texts, [16, 24–26].

2.2 Stochastic processes

Most of the phenomena observed in nature are in fact stochastic rather than deterministic. Therefore, a thorough knowledge of stochastic processes is important to gain. Master equations are the equations that describe the dynamics of stochastic systems which inherent a randomness.

2.2.1 Master equation

In this section, we are going to motivate the master equation with conceptual arguments by leaving the mathematical details of the derivation to textbooks, [23, 27]. A random motion can have values $x_1, x_2, ..., x_n, ...$ at times $t_1, t_2, ..., t_n, ...$ of a time-dependent random variable $x(t)$ so that joint probability densities can be written as,

$$P_n(x_1, t_1; x_2, t_2; ...; x_n, t_n), \qquad n = 1, 2, ... \tag{2.2.1}$$

Stochastic processes are always represented by stochastic variables changing in time. So, just a single realization of a stochastic process is a trajectory $x(t)$ as a function of time. If one writes Eq. (2.1.3) as,

$$P_n(x_1, t_1; x_2, t_2; ...; x_n, t_n)dx_1dx_2...dx_n, \qquad n = 1, 2, ... \tag{2.2.2}$$

we mean a sequence or hierarchy of probability distributions. Here, $P_1(x_1,t_1)dx_1$ is a time-dependent probability of first order to measure the value x_1 within $[x_1, x_1+dx_1]$ at time t_1. $P_2(x_2,t_2)dx_2$ is the probability of second order and so on for higher terms. Eq. (2.2.2) expresses the overall description of a stochastic process. A dynamical stochastic Markov process states the dependency of a measurement value x_2 at time t_2 only on the previous measurement value of x_1 at t_1. This lets conditional probabilities get in the picture. In fact these conditional probabilities represent the transitions between two neighbouring events in a stochastic process. For example, the conditional probability $P_2(x',t'|x,t)$ is called the transition probability from x at t to x' at t'. One can determine the whole hierarchy of probabilities by using these transition probabilities for Markov processes,

$$\begin{aligned} &P_n(x_n,t_n|x_{n-1},t_{n-1};...;x_1,t_1) = P_2(x_n,t_n|x_{n-1},t_{n-1}),\\ &P_2(x_1,t_1;x_2,t_2) = P_2(x_2,t_2|x_1,t_1)P_1(x_1,t_1). \end{aligned} \tag{2.2.3}$$

Eq. (2.2.3) enables us to calculate all higher probabilities starting from $P_1(x_1,t_1)$ which is unique to a Markov process. Then by a series of calculations [27], one can end up with

$$\frac{\partial}{\partial t}P_1(x,t) = \int w(x,x',t)P_1(x',t)dx' - \int w(x',x,t)P_1(x,t)dx', \tag{2.2.4}$$

where $P_1(x,t)$ is the probability distribution of first order, $w(x,x',t)$ is transition rate from x' to x and $w(x',x,t)$ is transition rate from x to x'. This is the master equation in integral form. One can write down its discrete form,

$$\frac{\partial}{\partial t}P(\bar{x},t) = \sum_{\bar{x}'\neq\bar{x}} \left[w(\bar{x},\bar{x}')P(\bar{x}',t) - w(\bar{x}',\bar{x})P(\bar{x},t)\right], \tag{2.2.5}$$

where $P(\bar{x},t) \equiv P(x_1,x_2,...,x_n,t)$. Master equation is a gain-loss equation where gain and loss are determined via the transition rates among probability distributions and it reflects how probability distributions change randomly in time. It can also be interpreted as a local balance for the probability densities for a distribution via normalization condition which dictates the total probability should be one:

$$\int P(x,t)dx = 1. \tag{2.2.6}$$

By solving this so to speak evolution equation, we can determine the relaxation from a chosen starting probability distribution $P(x,t=0)$ to some final probability distribution $P(x,t\to\infty)$. Additionally, the linearity of master equation is based on the assumption that the dynamics of the process are Markovian, so that the transition probabilities w do not depend on the history of the process. The underlying system is supposed to be memoryless.

We will be deriving a master equation for the cavity density matrix in the following chapters, because our stochastic system is the cavity interacting with an atomic reservoir for a sufficiently long time to be able to come to steady-state. For this problem, the state space of the stochastic variable, which is the cavity states, is discrete since a cavity consists of Fock states, $n \geq 0$. Then the master equation for the time evolution of the probabilities $P(n,t)$,

$$\frac{dP(n,t)}{dt} = \sum_{n' \neq n} \left[w(n,n')P(n',t) - w(n',n)P(n,t) \right], \tag{2.2.7}$$

where $w(n',n) \geq 0$ are rate constants (due to Markovian dynamics) for transitions from n to another $n' \neq n$. When the initial conditions (probabilities) $P(n, t=0)$ for $n = 0, 1, 2, ..., N$ and boundary conditions at $n = 0$ and $n = N$ are given, time evolution of probabilities from the start to the long-time limit $t \to \infty$ can be solved. Analysis of Eq. (2.2.7) reveals that the first term at the right hand side of the equation is the inflow current to state n due to transitions from other states n', whereas the second term is the outflow current due to opposite transitions from n to n'. In our case, the boundary conditions are set so that the cavity will be thermal both initially and finally, because thermodynamics require thermal states. In fact, when we inject coherent reservoirs and let the system evolve in time, we will witness an increase in the mean photon number via vanishing coherence, [3] and leaving the cavity thermal at the end of the process.

Finally, we are going to discuss stationarity, which is an important concept that tells about the thermalization of the system. A stochastic process can reach to a steady state or thermal equilibrium in thermodynamics when the change in probability does not vary with respect to time,

$$\frac{dP(n,t)}{dt} = 0 \to P(n,t) = P^e. \tag{2.2.8}$$

Then the stationary master equation is,

$$0 = \sum_{n' \neq n} \left[w(n,n')P^e(n') - w(n',n)P^e(n) \right]. \tag{2.2.9}$$

Eq. (2.2.9) expresses a local probability conservation, where the summation of the inflow and outflow of currents for probability distributions are balanced. A stronger constraint, the so-called detailed balance condition, requires that each of the inflow and outflow of currents are balanced,

$$0 = w(n,n')P^e(n') - w(n',n)P^e(n), \tag{2.2.10}$$

after a sufficiently long time, $t \to \infty$. Eq. (2.2.10), namely the condition of detailed balance, will be extremely important for us, because exactly this equation represents

the thermal equilibrium.

2.2.2 Lindblad quantum master equation

Each model has its own master equation, so in that sense master equation is not unique. However there are some specific forms of master equations that appear in certain types of problems. Lindblad form of master equation is one of those. Lindblad master equation is also the form that we come across throughout this thesis research.

A master equation of Lindblad form has the structure, [28],

$$\dot{\rho} = -i\left[H, \rho\right] + \sum_{j} \left(L_j \rho L_j^{\dagger} - \frac{1}{2} \left\{ L_j^{\dagger} L_j, \rho \right\} \right), \tag{2.2.11}$$

where L_j's are Lindblad operators. The commutator term with Hamiltonian in Eq. (2.2.11) gives the unitary evolution, while the other terms represent nonunitary or dissipative evolution. In our master equations, the random injections of atoms will create Lindblad type of dissipation terms. So, the cavity will lose energy (cooling) or gain energy (thermalization) through the loss-gain channels of atomic reservoir.

2.3 Modelling a heat reservoir as atoms

A heat reservoir is an ensemble of infinitely many modes. If the operator that defines the system is S and the operator of each mode of reservoir is R, the interaction Hamiltonian,

$$H_{\text{int}} = \sum_{j} g_j S R_j, \tag{2.3.1}$$

where SR_j describes a process of interaction. One should note that g_j is coupling strength of j^{th} mode of reservoir. The coupling strengths are assumed to be different for each mode due to the random distribution of atoms and molecules in a real reservoir. Therefore, reservoirs are mostly modelled with quantum harmonic oscillators. However in our case, reservoir is atoms. Atomic modelling of a reservoir is in fact subtle with intricate details. Thus, we will only discuss it conceptually.

By ergodic theorem it is possible to represent the phase space average of a system's degrees of freedom with a time average of its degrees of freedom, [29]. Therefore, we can transform a space-related problem to a time-related problem as long as certain ergodicity conditions are satisfied. Injections of atoms continuously mimics the reservoir behaviour due to ergodic theorem. However, there is another point to make as well:

varying coupling strengths, g_j. In fact our model can mimic this behaviour too if we send the atoms into the cavity randomly so that the arrival of atoms is carried out in a Poissonian distribution, [30].

Chapter 3

Tavis-Cummings Model for Interaction

Thermalization of a cavity with correlated atoms is a time-dependent problem. As in any time-dependent quantum mechanical problem, we need to calculate an evolution operator, which will evolve the system state in time. For this purpose, one should first choose the interaction model. Since we assume that the interaction between the cavity and the atoms is weak enough, we apply Rotating Wave Approximation (RWA) to the interaction term, which reduces the Rabi Hamiltonian to the Jaynes-Cummings Hamiltonian. A more detailed discussion and calculation of this reduction can be found in my previous thesis report, [31]. In this chapter, we are going to start from dressed states of the Jaynes-Cummings (JC) Model and we will extend the formalism of JC Model to Tavis-Cummings (TC) Model, which consists of multiple atoms instead of only one. Since thermalization problem requires an evolution operator to run the quantum master equation, we are going to derive the evolution operators to be used. It should be noted that as the complexity increases with the number of atoms used, the approximate form of the evolution operator will suffice. Because the problem under study is thermalization of a cavity with fast transitions of correlated atoms. Therefore, in principle we do not need the exact forms of evolution operators. In fact, we are going to discuss the problems arising in the calculations of the exact forms, but we will be limited to a discussion only.

3.1 Jaynes-Cummings Model

The Jaynes-Cummings model is a quantum electrodynamical description of the interaction between a two-level system and a single mode cavity, [32].

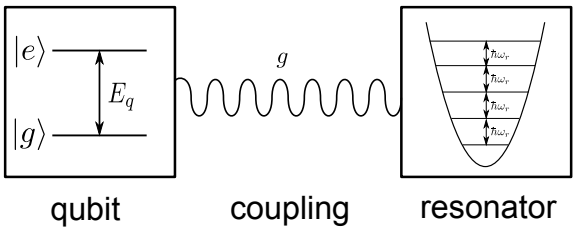

FIGURE 3.1: A schematic for the Jaynes-Cummings Model, represents an interaction between a two-level system and a quantum harmonic oscillator.

A schematic of the interaction can be seen in Fig. 3.1. The JC Hamiltonian will be composed of three parts:

$$\hat{H}_{JC} = \hat{H}_{qb} + \hat{H}_r + \hat{H}_I. \tag{3.1.1}$$

$\hat{H}_{qb}$ is the Hamiltonian of the qubit or two-level system, $\hat{H}_r$ is the Hamiltonian of the resonator and finally $\hat{H}_I$ is the interaction Hamiltonian. The Hamiltonian for the qubit can be written in general as,

$$\hat{H}_{qb} = \frac{1}{2}\hbar\omega_{qb}\hat{\sigma}_z, \tag{3.1.2}$$

where $\hat{\sigma}_z$ is the Pauli Z matrix and the terms in the diagonal represent two independent levels. The Hamiltonian for the resonator is that of a quantum harmonic oscillator, written in terms of annihilation and creation operators,

$$\hat{H}_r = \hbar\omega_r\hat{a}^\dagger\hat{a}, \tag{3.1.3}$$

where we did not take the zero-point energy, simply because we are interested in relative energy values here. Lastly for the interaction Hamiltonian, we should introduce atomic transition operators in a two-level system, which enable the transitions from ground to excited state (or vice versa):

$$\hat{\sigma}_+ \equiv |e\rangle\langle g|, \qquad \hat{\sigma}_- \equiv |g\rangle\langle e|. \tag{3.1.4}$$

The electrodynamic interaction between the two systems can be realized through electric dipole coupling, which can be written as

$$\hat{H}_I = -\hat{\mathbf{d}}\cdot\hat{\mathbf{E}}, \tag{3.1.5}$$

where $\hat{\mathbf{d}}$ is a dipole operator which consists of atomic transition operators, Eq. (3.1.4), and a coupling constant, g. Similarly, the quantized electric field can be written in terms

of photon creation and annihilation operators. Therefore, when we gather all terms and apply the so-called rotating wave approximation (RWA), Jaynes-Cummings Hamiltonian becomes

$$\hat{H} = \frac{1}{2}\hbar\omega_{qb}\hat{\sigma}_z + \hbar\omega_r\hat{a}^\dagger\hat{a} + \hbar g\left(\hat{\sigma}_+\hat{a} + \hat{\sigma}_-\hat{a}^\dagger\right). \tag{3.1.6}$$

One can diagonalize Hamiltonian (3.1.6) and derive the eigenvalues as,

$$E_\pm = \hbar\omega_r\left(n - \frac{1}{2}\right) \pm \frac{1}{2}\sqrt{\hbar^2\left(4g^2n + \delta^2\right)}, \tag{3.1.7}$$

where $\delta \equiv (\omega_{qb} - \omega_r)$ is the frequency detuning and $n = a^\dagger a$ is excitation. We can choose the normalized eigenvectors as,

$$|n,+\rangle = \cos(\theta/2)\,|\psi_{1n}\rangle + \sin(\theta/2)\,|\psi_{2n}\rangle\,, \tag{3.1.8}$$

$$|n,-\rangle = -\cos(\theta/2)\,|\psi_{1n}\rangle + \sin(\theta/2)\,|\psi_{2n}\rangle\,, \tag{3.1.9}$$

where,

$$\theta = \tan^{-1}\left(\frac{2g\sqrt{n}}{\delta}\right). \tag{3.1.10}$$

These normalized eigenvectors are the dressed states of the JC Hamiltonian with the corresponding energy eigenvalues $E_\pm$.

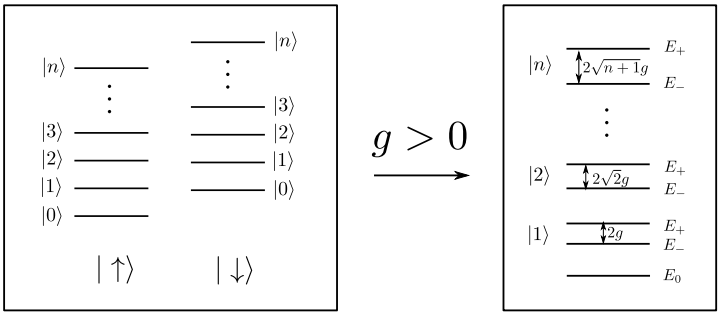

FIGURE 3.2: A schematic which shows the uncoupled Jaynes-Cummings states when $g = 0$ and dressed states when $g > 0$.

The schematic 3.2 shows the uncoupled states when there is no coupling and the formation of the dressed states with a splitting value of the Rabi frequency when the g coupling is on and at resonance.

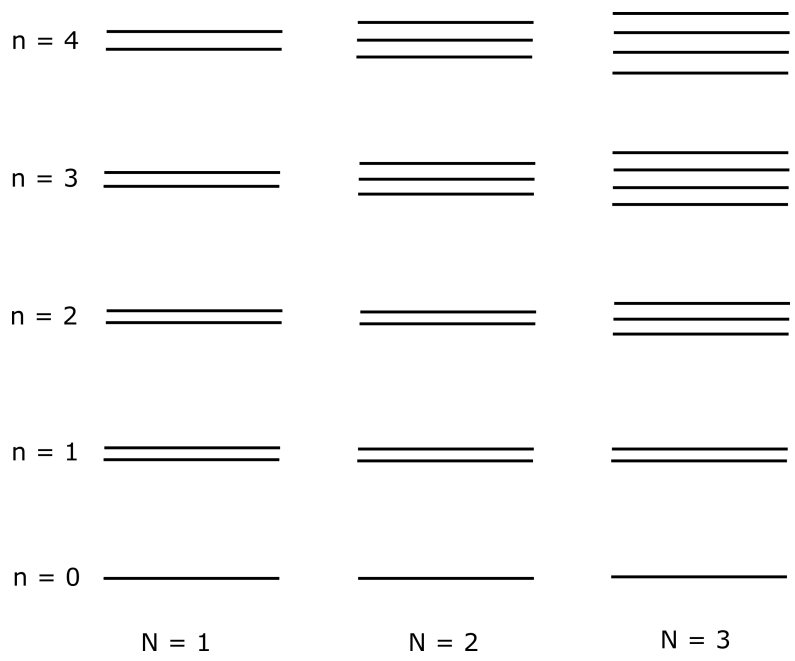

FIGURE 3.3: The energy level structure of Tavis-Cummings Model for different atom numbers $N = 1, 2, 3$.

3.2 Tavis-Cummings Model

Tavis-Cummings Model is a generalization of Jaynes-Cummings Model to N qubits, [33]. We can write down the Hamiltonian as,

$$H_{TC} = H_a + H_c + H_{\text{int}}, \tag{3.2.1}$$

where $H_a = \hbar\omega_a \sum_{j=1}^{N} \sigma_j^z$, $H_c = \hbar\omega_c a^\dagger a$ and $H_{\text{int}} = \hbar g \sum_{j=1}^{N} \left(a\sigma_j^+ + a^\dagger \sigma_j^-\right)$. Here σ^z is the z Pauli operator, $a, a^\dagger$ are annihilation and creation operators for cavity field and σ^+, σ^- are raising and lowering operators for TLATs, respectively. Additionally, we assume resonance condition throughout thesis, so that $\omega_a = \omega_c$. One can refer to [34] for the eigenstructure of two-atom Tavis-Cummings Model. Let us note that there are only three dressed states for a specific photon number in the cavity when Tavis-Cummings Model for two coupled atoms is used due to two degenerate states, $|eg\rangle$ and $|ge\rangle$. Since we are not going to use the dressed states and resort to interaction picture with only calculating evolution operators in this research, we are not presenting an analysis of Tavis-Cummings Model here. One can see the effects of degenerate levels in evolution operator, as well. For 3-atom case, where this thesis research is focused, there are two-fold degeneracy of which the first fold, $|egg\rangle$, $|geg\rangle$ and $|gge\rangle$ and the second fold, $|eeg\rangle$, $|ege\rangle$ and $|gee\rangle$. Therefore, one can deduce that when there are more than two photons in the cavity field, the eigenstates of 3-atom Tavis-Cummings Model will be formed in

manifolds of four levels whose energy level spacings change as the photon number varies, Fig. 3.3.

3.3 Calculating the evolution operators

Cavity thermalization problem has an intrinsic time-dependent nature. This forces us to calculate the evolution operator of a specific Tavis-Cummings interaction explicitly if it is possible to compute or approximate. We are going to deal with the derivation of exact and approximated forms of evolution operators for different cases in this section.

3.3.1 One atom within a cavity

Jaynes-Cummings Model consists of a cavity and an atom as previously mentioned in Sec. 3.1. Evolution operator of such an interaction will be of the following form:

$$\hat{U}(t) \equiv \exp(-i\hat{H}_{\text{int}}t), \tag{3.3.1}$$

where $\hat{H}_{\text{int}} = g\left(\sigma_+ a + \sigma_- a^\dagger\right)$. The two-level atom spans a space of 2 dimensions. Then, we can restate the evolution operator as,

$$\hat{U}(t) = \exp(-igtP), \tag{3.3.2}$$

where P stands for product and it is explicitly,

$$P_{1/2} = \begin{pmatrix} 0 & a \\ a^\dagger & 0 \end{pmatrix} \tag{3.3.3}$$

In order to calculate the exponential of Eq. (3.3.3), one needs to calculate the n^{th} power of Eq. (3.3.3). Then,

$$P_{1/2}^2 = \begin{pmatrix} aa^\dagger & 0 \\ 0 & a^\dagger a \end{pmatrix} = \begin{pmatrix} N+1 & 0 \\ 0 & N \end{pmatrix}. \tag{3.3.4}$$

Now what is important is the diagonal and operator-free form of Eq. (3.3.4). Because, in the end one should be calculating the following series expansion:

$$\exp(-itgP_{1/2}) = \sum_{n=0}^{\infty} \frac{(-1)^n}{(2n)!}(tg)^{2n} P_1^{2n} - i\sum_{n=0}^{\infty} \frac{(-1)^n}{(2n+1)!}(tg)^{2n+1} P_1^{2n+1}. \tag{3.3.5}$$

Eq. (3.3.5) contains n^{th} power of $P_{1/2}^2$, which can be calculated without any problems due to diagonal nature of $P_{1/2}^2$. Additionally, we need $P_{1/2}^{2n+1}$, but this is not a problem either. Because it can be written as $P_{1/2}^{2n}P_{1/2} = P_{1/2}P_{1/2}^{2n}$ and gives,

$$P_{1/2}^3 = \begin{pmatrix} 0 & (N+1)a \\ Na^\dagger & 0 \end{pmatrix}. \tag{3.3.6}$$

Therefore, one can easily obtain the closed form of Eq. (3.3.5),

$$U_1(t) = \begin{pmatrix} \cos\left(gt\sqrt{N+1}\right) & -i\frac{a\sin\left(gt\sqrt{N+1}\right)}{\sqrt{N+1}} \\ -i\frac{\sin\left(gt\sqrt{N}\right)a^\dagger}{\sqrt{N}} & \cos\left(gt\sqrt{N}\right) \end{pmatrix}. \tag{3.3.7}$$

This case was easy, so that we achieved to find an exact form. Let us also note the approximate form for the next chapters,

$$U_1(t) \approx \begin{pmatrix} 1-\frac{1}{2}(gt)^2(N+1) & -iagt \\ -igta^\dagger & 1-\frac{1}{2}(gt)^2N \end{pmatrix}. \tag{3.3.8}$$

3.3.2 Two atoms within a cavity

What about increasing the number of atoms? The method is obvious: we should find out the diagonal matrices in order to calculate the exponential evolution operator. In this section, we will discuss the problems related to exact forms of evolution operators while deriving the exact forms. Afterwards, we are going to introduce a general technique to make the calculation of evolution operator easier.

We can write the interaction matrix as,

$$\hat{H}_{\text{int}} = g\begin{pmatrix} 0 & a & a & 0 \\ a^\dagger & 0 & 0 & a \\ a^\dagger & 0 & 0 & a \\ 0 & a^\dagger & a^\dagger & 0 \end{pmatrix}. \tag{3.3.9}$$

Let us write it as $gP_2 = H_{\text{int}}$ and take the square of P_2:

$$P_2^2 = \begin{pmatrix} 2N+2 & 0 & 0 & 2a^2 \\ 0 & 2N+1 & 2N+1 & 0 \\ 0 & 2N+1 & 2N+1 & 0 \\ 2\left(a^\dagger\right)^2 & 0 & 0 & 2N \end{pmatrix}. \tag{3.3.10}$$

Now it is important to realize that P_2^2 is not diagonal and operator-free, which is going to trigger problems when Eq. (3.3.10) is substituted into Eq. (3.3.5). We can observe that $P_2 P_2^2 = P_2^2 P_2$:

$$P_2^3 = \begin{pmatrix} 0 & 2(2N+3)a & 2(2N+3)a & 0 \\ 2(2N+1)a^\dagger & 0 & 0 & 2(2N+1)a \\ 2(2N+1)a^\dagger & 0 & 0 & 2(2N+1)a \\ 0 & 2(2N-1)a^\dagger & 2(2N-1)a^\dagger & 0 \end{pmatrix}, \tag{3.3.11}$$

However, as one can see even the n^{th} matrix power of P_2 will be containing operators and will not be in diagonal form. Nevertheless, it is possible to write down a few powers of the matrix by taking the non-commutative algebra into account and see the pattern in order to derive the evolution operator. However, this is indeed a cumbersome calculation especially when the atom space is greater than two. Therefore, in order to exploit the practicality of a series expansion, we would like to diagonalize the P_2^2 matrix. This brings us to a new problem: how can we make diagonalization when the elements are infinite dimensional operators?

Ref. [22] introduces a method coined as Quantum Diagonalization to compute the evolution operators by exploiting the series expansions. Since the analysis of this method is beyond this thesis, we are going to use the results when needed. However an educated inspection to P_2^2 matrix, (3.3.10) can suffice right now. See the following diagonal matrix results the same P_2^3, Eq. (3.3.11).

$$D_2 = \begin{pmatrix} 2(2N+3) & 0 & 0 & 0 \\ 0 & 2(2N+1) & 0 & 0 \\ 0 & 0 & 2(2N+1) & 0 \\ 0 & 0 & 0 & 2(2N-1) \end{pmatrix}. \tag{3.3.12}$$

Then we can make use of the series expansion,

$$\exp(-itgP_2) = \mathbb{I} + \sum_{n=1}^{\infty} \frac{(-1)^n}{(2n)!}(tg)^{2n} P_2^{2n} - i \sum_{n=0}^{\infty} \frac{(-1)^n}{(2n+1)!}(tg)^{2n+1} P_2^{2n+1}, \tag{3.3.13}$$

by substituting $P_2^{2n} = D_2^{n-1} P_2^2$ and $P_2^{2n+1} = D_2 P_2$. We are going to have,

$$U_2(t) = \exp(-itgP_2) =$$

$$\begin{pmatrix} \frac{N+(N+1)\cos\left(g\sqrt{4N+6}t\right)+2}{2N+3} & \frac{-ia\sin\left(g\sqrt{4N+6}t\right)}{\sqrt{4N+6}} & \frac{-ia\sin\left(g\sqrt{4N+6}t\right)}{\sqrt{4N+6}} & \frac{a^2\left(\cos\left(g\sqrt{4N+6}t\right)-1\right)}{2N+3} \\ \frac{-i\sin\left(g\sqrt{4N+2}t\right)a^\dagger}{\sqrt{4N+2}} & \frac{\cos\left(g\sqrt{4N+2}t\right)+1}{2} & \frac{\cos\left(g\sqrt{4N+2}t\right)-1}{2} & \frac{-ia\sin\left(g\sqrt{4N+2}t\right)}{\sqrt{4N+2}} \\ \frac{-i\sin\left(g\sqrt{4N+2}t\right)a^\dagger}{\sqrt{4N+2}} & \frac{\cos\left(g\sqrt{4N+2}t\right)-1}{2} & \frac{\cos\left(g\sqrt{4N+2}t\right)+1}{2} & \frac{-ia\sin\left(g\sqrt{4N+2}t\right)}{\sqrt{4N+2}} \\ \frac{\left(\cos\left(g\sqrt{4N-2}t\right)-1\right)\left(a^\dagger\right)^2}{2N-1} & \frac{-i\sin\left(g\sqrt{4N-2}t\right)a^\dagger}{\sqrt{4N-2}} & \frac{-i\sin\left(g\sqrt{4N-2}t\right)a^\dagger}{\sqrt{4N-2}} & \frac{\cos\left(g\sqrt{4N-2}t\right)N+N-1}{2N-1} \end{pmatrix}. \tag{3.3.14}$$

3.3.2.1 Divide and Conquer Technique

As the dimension of Hilbert space increases, the algebraic calculations become tedious. The case for two atoms may be handled, however applying the same procedure for exact three atom case might not produce results, [22]. Therefore, we are going to use a method that we named as 'Divide and Conquer Technique' for the problems involving higher numbers of atoms.

This technique implements the transformation of spin product states to spin sum states, so that one can tackle the problem in smaller units. For example for the case with two atoms, we will utilize the transformation of $\frac{1}{2} \otimes \frac{1}{2} = 0 \oplus 1$. The transformation matrix that does this is,

$$T = \begin{pmatrix} 0 & 1 & 0 & 0 \\ \frac{1}{\sqrt{2}} & 0 & \frac{1}{\sqrt{2}} & 0 \\ -\frac{1}{\sqrt{2}} & 0 & \frac{1}{\sqrt{2}} & 0 \\ 0 & 0 & 0 & 1 \end{pmatrix}, \tag{3.3.15}$$

so that,

$$T^\dagger P_2 T = \begin{pmatrix} 0 & 0 & 0 & 0 \\ 0 & 0 & \sqrt{2}a & 0 \\ 0 & \sqrt{2}a^\dagger & 0 & \sqrt{2}a \\ 0 & 0 & \sqrt{2}a^\dagger & 0 \end{pmatrix} = \begin{pmatrix} P_0 & & \\ & & \\ & & P_{2/2} \end{pmatrix}, \tag{3.3.16}$$

where P_2 originates from Eq. (3.3.9). Now we will apply the same procedure in previous part to $P_{2/2}$. So, similar calculations lead to,

$$P_{2/2}^2 = \begin{pmatrix} 2(N+1) & 0 & 2a^2 \\ 0 & 4N+2 & 0 \\ 2\left(a^\dagger\right)^2 & 0 & 2N \end{pmatrix}. \tag{3.3.17}$$

One can easily check out the diagonal matrix given below gives expected results:

$$P_{2/2}^3 = \begin{pmatrix} 2(2N+3) & 0 & 0 \\ 0 & 2(2N+1) & 0 \\ 0 & 0 & 2(2N-1) \end{pmatrix} P_{2/2}. \tag{3.3.18}$$

Then by exploiting the following relations,

$$\begin{aligned} P_{2/2}^{2n} &= D^{n-1} P_{2/2}^2, \quad n \geq 1, \\ P_{2/2}^{2n+1} &= D^n P_{2/2}, \quad n \geq 0, \end{aligned} \tag{3.3.19}$$

and Eq. (3.3.13), where D is the diagonal matrix, one can end up with,

$$\mathrm{e}^{-igtP_{2/2}} = \mathbb{I} + \begin{pmatrix} -\frac{2(N+1)\sin^2\left(g\sqrt{N+\frac{3}{2}}t\right)}{2N+3} & -\frac{ia\sin\left(g\sqrt{4N+6}t\right)}{\sqrt{2N+3}} & \frac{a^2\left(\cos\left(g\sqrt{4N+6}t\right)-1\right)}{2N+3} \\ -\frac{i\sin\left(g\sqrt{4N+2}t\right)a^\dagger}{\sqrt{2N+1}} & \cos\left(g\sqrt{4N+2}t\right)-1 & -\frac{ia\sin\left(g\sqrt{4N+2}t\right)}{\sqrt{2N+1}} \\ \frac{\left(\cos\left(g\sqrt{4N-2}t\right)-1\right)\left(a^\dagger\right)^2}{2N-1} & -\frac{i\sin\left(g\sqrt{4N-2}t\right)a^\dagger}{\sqrt{2N-1}} & \frac{N\left(\cos\left(g\sqrt{4N-2}t\right)-1\right)}{2N-1} \end{pmatrix}. \tag{3.3.20}$$

Then it is clear that by applying the transformation back, $TP_2T^\dagger$, one can find out the evolution operator for 2 atoms, Eq. (3.3.14).

Let us now note the approximate form of the evolution operator for 2 atoms in the instantaneous interaction limit, which requires a substitution of $\cos\theta = 1 - \theta^2/2!$ and $\sin\theta = \theta$.

$$U_2(t) \approx \begin{pmatrix} 1-g^2(N+1)t^2 & -iagt & -iagt & -a^2g^2t^2 \\ -igta^\dagger & \frac{1}{2}\left(2-g^2(2N+1)t^2\right) & -\frac{1}{2}g^2(2N+1)t^2 & -iagt \\ -igta^\dagger & -\frac{1}{2}g^2(2N+1)t^2 & \frac{1}{2}\left(2-g^2(2N+1)t^2\right) & -iagt \\ -g^2t^2\left(a^\dagger\right)^2 & -igta^\dagger & -igta^\dagger & 1-g^2Nt^2 \end{pmatrix}. \tag{3.3.21}$$

3.3.3 Three atoms within a cavity

Evolution operator due to interaction between three atoms and a cavity will be of the following form:

$$U(t) \equiv \exp(-iH_{\mathrm{int}}t) = \exp(-igtP_3), \tag{3.3.22}$$

where P_3 stands for product:

$$P_3 = \begin{pmatrix} 0 & a & a & 0 & a & 0 & 0 & 0 \\ a^\dagger & 0 & 0 & a & 0 & a & 0 & 0 \\ a^\dagger & 0 & 0 & a & 0 & 0 & a & 0 \\ 0 & a^\dagger & a^\dagger & 0 & 0 & 0 & 0 & a \\ a^\dagger & 0 & 0 & 0 & 0 & a & a & 0 \\ 0 & a^\dagger & 0 & 0 & a^\dagger & 0 & 0 & a \\ 0 & 0 & a^\dagger & 0 & a^\dagger & 0 & 0 & a \\ 0 & 0 & 0 & a^\dagger & 0 & a^\dagger & a^\dagger & 0 \end{pmatrix}. \tag{3.3.23}$$

If we apply a transformation matrix, which in fact transforms from product basis to total spin basis, $\frac{1}{2} \otimes \frac{1}{2} \otimes \frac{1}{2} = \frac{1}{2} \oplus \frac{1}{2} \oplus \frac{3}{2}$ to P_3, we obtain the interaction matrix in the block diagonal form:

$$T^\dagger P_3 T = \begin{pmatrix} 0 & a & 0 & 0 & 0 & 0 & 0 & 0 \\ a^\dagger & 0 & 0 & 0 & 0 & 0 & 0 & 0 \\ 0 & 0 & 0 & a & 0 & 0 & 0 & 0 \\ 0 & 0 & a^\dagger & 0 & 0 & 0 & 0 & 0 \\ 0 & 0 & 0 & 0 & 0 & \sqrt{3}a & 0 & 0 \\ 0 & 0 & 0 & 0 & \sqrt{3}a^\dagger & 0 & 2a & 0 \\ 0 & 0 & 0 & 0 & 0 & 2a^\dagger & 0 & \sqrt{3}a \\ 0 & 0 & 0 & 0 & 0 & 0 & \sqrt{3}a^\dagger & 0 \end{pmatrix} = \begin{pmatrix} P_{1/2} & & & \\ & P_{1/2} & & \\ & & P_{3/2} & \end{pmatrix}. \tag{3.3.24}$$

Transformation matrix is given by:

$$T = \begin{pmatrix} 0 & 0 & 0 & 0 & 1 & 0 & 0 & 0 \\ \frac{1}{\sqrt{2}} & 0 & \frac{1}{\sqrt{6}} & 0 & 0 & \frac{1}{\sqrt{3}} & 0 & 0 \\ -\frac{1}{\sqrt{2}} & 0 & \frac{1}{\sqrt{6}} & 0 & 0 & \frac{1}{\sqrt{3}} & 0 & 0 \\ 0 & 0 & 0 & \sqrt{\frac{2}{3}} & 0 & 0 & \frac{1}{\sqrt{3}} & 0 \\ 0 & 0 & -\sqrt{\frac{2}{3}} & 0 & 0 & \frac{1}{\sqrt{3}} & 0 & 0 \\ 0 & \frac{1}{\sqrt{2}} & 0 & -\frac{1}{\sqrt{6}} & 0 & 0 & \frac{1}{\sqrt{3}} & 0 \\ 0 & -\frac{1}{\sqrt{2}} & 0 & -\frac{1}{\sqrt{6}} & 0 & 0 & \frac{1}{\sqrt{3}} & 0 \\ 0 & 0 & 0 & 0 & 0 & 0 & 0 & 1 \end{pmatrix}. \tag{3.3.25}$$

We already found out the expression for $\exp(-itgP_{1/2})$ as Eq. (3.3.7) for exact form and Eq. (3.3.8) for approximate form. So, after finding $\exp(-itgP_{3/2})$, we are going to write the transformed operator in block-diagonal form and reapply the transformation matrix to find out the final form of the evolution operator.

Calculating $P_{3/2}$ is a more challenging problem. In fact we applied only brute force to calculate the approximate form of $P_{3/2}$ and confirmed that the exact form given in [22] is true. The reader should refer there to see the exact form of $P_{3/2}$ in a properly written way. Since we only need an approximated version of evolution operator in this study, we will write that down,

$$\exp(igtP_{3/2}) \approx \frac{1}{2}\mathbb{I} - \begin{pmatrix} 3(gt)^2(N+1) & -i\sqrt{3}agt & -\sqrt{3}a^2(gt)^2 & 0 \\ -i\sqrt{3}gta^\dagger & (gt)^2(7N+4) & -2iagt & -\sqrt{3}a^2g^2t^2 \\ -\sqrt{3}(gt)^2\left(a^\dagger\right)^2 & -2igta^\dagger & gt(7N+3) & -i\sqrt{3}agt \\ 0 & -\sqrt{3}(gt)^2\left(a^\dagger\right)^2 & -i\sqrt{3}gta^\dagger & 3(gt)^2N \end{pmatrix}. \tag{3.3.26}$$

Then one can combine these smaller parts of the evolution operator, Eq. (3.3.24) and apply the transformation matrix Eq. (3.3.25) back to derive the approximated version of the evolution operator elements as,

$$\begin{aligned}
&U_{11} = \frac{1}{2}\left(2 - 3(gt)^2(a^\dagger a + 1)\right), \\
&U_{21} = U_{31} = U_{42} = U_{62} = U_{43} = U_{73} = U_{84} = U_{65} = U_{75} = U_{86} = U_{87} = -igta^\dagger, \\
&U_{41} = U_{61} = U_{71} = U_{82} = U_{83} = U_{85} = -(gt)^2\left(a^\dagger\right)^2, \\
&U_{12} = U_{13} = U_{14} = U_{15} = U_{26} = U_{56} = U_{37} = U_{57} = U_{48} = U_{68} = U_{78} = -iagt, \\
&U_{22} = U_{33} = U_{55} = 1 - \frac{1}{2}(gt)^2(3a^\dagger a + 2), \\
&U_{32} = U_{52} = U_{23} = U_{53} = U_{64} = U_{74} = U_{25} = U_{35} = U_{46} = U_{76} = U_{47} = U_{67} = -\frac{1}{2}(gt)^2(2a^\dagger a + 1), \\
&U_{14} = U_{16} = U_{17} = U_{28} = U_{38} = U_{58} = -a^2(gt)^2, \\
&U_{44} = U_{66} = U_{77} = 1 - \frac{1}{2}(gt)^2(3a^\dagger a + 1), \\
&U_{88} = 1 - \frac{3}{2}(gt)^2a^\dagger a, \\
&U_{81} = U_{72} = U_{63} = U_{54} = U_{45} = U_{36} = U_{27} = U_{18} = 0.
\end{aligned} \tag{3.3.27}$$

One can always work out the approximated versions of the evolution operators by brute force and make sure that the method is working fine.

Chapter 4

Quantum Thermodynamics

Understanding how thermalization occurs between quantum mechanical objects is significant to describe the working mechanisms of especially quantum heat engines (QHE),[35] accurately. Because just like classical heat engines, QHEs have thermodynamic cycles of isothermal, isochoric and adiabatic processes. Therefore, thermalization of a cavity is an essential part of a QHE to produce useful work out of quantum matter.

In this section, we are going to give a brief introduction to quantum heat engines focusing on the quantum-classical transitions in a quantum thermodynamic cycle as well as describing the role of thermalization on extracting work. All in all, we are going to show that QHE is an important motivation to study thermalization in quantum mechanics.

4.1 Basic classical and quantum thermodynamic processes

In this section, we are going to review the basic thermodynamic concepts and processes both classically and quantum mechanically to draw some parallels between the two and develop an intuition regarding the quantum version. This section follows the discussions in [4].

4.1.1 The working substance

First law of thermodynamics states,

$$dU = dQ + dW, \tag{4.1.1}$$

so that to extract work from a system, one should first feed it with a fuel, which will pump heat to the system. This fact leads us to ask the question of what the working

substance is for systems. For classical heat engines, the fuel can be traditionally coal, oil, natural gas etc. For quantum mechanical heat engines, the working substance is atoms with finite or infinite number of energy levels. The treatment of quantum heat engines started with a two-level and three-level with a degenerate ground level atomic fuels (reservoirs-heat baths), [35], [3]. Additionally, there is a substantial research on multi-level atomic fuels of single atom [36] or many atoms with two energy levels [10]. This thesis research focuses on the analytical derivation of the device working with many two-level atomic reservoirs. In any case, the working substance is a multi-level atomic system with a Hamiltonian of,

$$H = \sum_n E_n \left|n\right\rangle \left\langle n\right|, \tag{4.1.2}$$

where E_n is the corresponding energy eigenvalue of n^{th} eigenstate. Then the internal energy of this quantum mechanical fuel is,

$$U = \langle H \rangle = \sum_n P_n E_n, \tag{4.1.3}$$

where P_n is the occupation probability of n^{th} eigenstate. Then we can state the quantum mechanical analogue of first law of thermodynamics:

$$dU = \sum_n (E_n dP_n + P_n dE_n). \tag{4.1.4}$$

It is clear that heat and work terms in classical thermodynamic equation correspond to these two terms seen at the right hand side of Eq. (4.1.4). The heat is related to entropy via $dQ = TdS$ and the general expression for entropy is $S = -k_B \sum_i P_i \ln P_i$. Therefore, we argue that the term with a differential in probability should be related to the heat term in the first law.

$$dQ = \sum_n E_n dP_n, \tag{4.1.5}$$

$$dW = \sum_n P_n dE_n. \tag{4.1.6}$$

In fact, this identification is intuitive because Eq. (4.1.6) states that to extract work, one should let the populations in energy levels change to obtain a nonzero eigenenergy difference. Recall that $dW = \sum_i X_i dx_i$ where x_i is the generalized coordinates and X_i is the generalized force conjugated to x_i. So, here a change in eigenenergies corresponds to a change in the generalized coordinates and the probabilities map to generalized forces in microscopic treatment of mechanical systems. To sum up, spontaneous emission and absorption phenomena of atoms will let a change in the populations of energy levels with certain emission and absorption rates, P_n respectively. By emissions and absorptions of

atomic reservoirs, the engine will be able to generate nonzero work output.

4.1.2 Isothermal processes

Classically in an isothermal process, the change in internal energy is zero, so that whole heat change during a cycle (between heat intake and entropy sink) is equal to produced work [37].

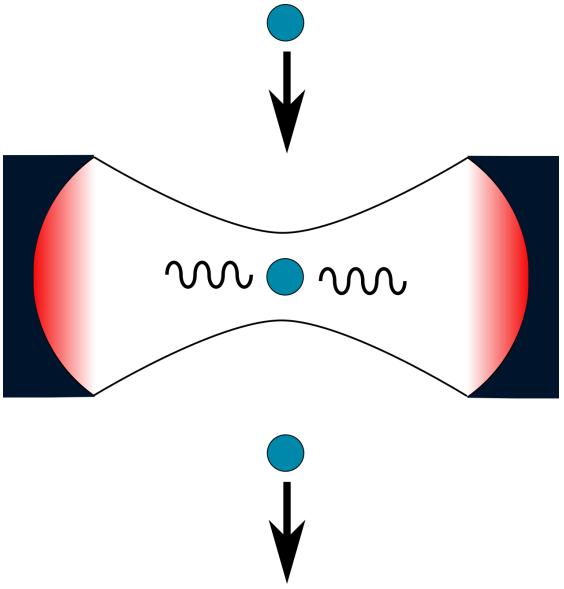

FIGURE 4.1: Model schematic of the quantum thermal interaction: atomic reservoir is injected into the cavity where the work is produced with generated photon number in cavity.

In quantum isothermal processes, the change in the internal energy is not necessarily zero. The injection of atomic reservoirs into the cavity represents the heat given to the system, whereas the emission and absorption processes that take place in atomic reservoirs during these injections is supposed to thermalize the cavity. After thermalization, work is produced through the mean photon number. Cavity thermalization means that the cavity is filled with thermal photons, whose radiation pressure is what does the work, [3]:

$$W = PV = \hbar\omega\bar{n}. \tag{4.1.7}$$

So, in more general words, just like in classical isothermal process, heat is absorbed and work is done by the system simultaneously in a quantum isothermal process. Quantum thermalization is an integral part of quantum isothermal process. A figure of the thermalization part of quantum isothermal process can be seen in Fig. 4.1. What does not change in a quantum isothermal process is the temperature of the reservoir throughout this process. So, for a two-level atomic reservoir, it is possible to write down its

temperature through Boltzmann distribution,

$$r = \frac{P_e}{P_g} = \exp\left(-\beta\omega(t)\right). \tag{4.1.8}$$

Therefore, we can state that the system should be thermalized with a temperature equal to the temperature of the reservoir at every instant in a sufficiently slow process, which is the defining condition for thermalization concept in thermodynamics. However, a problem arises with the question of temperature in multi-level atomic reservoirs and two-level atomic reservoirs with coherence. For such cases, definition of temperature has ambiguities. That is why an effective temperature is introduced for coherent two-level atomic reservoirs or nonequilibrium states:

$$T_{\text{eff}} = \frac{1}{k_B \beta_{\text{eff}}} = \frac{\omega(t)}{k_B} \left(\ln \frac{P_g}{P_e}\right)^{-1}. \tag{4.1.9}$$

In fact, Eq. (4.1.9) is exactly the same equation with Eq. (4.1.8), however the definition is seriously altered. Since a coherent reservoir is more energetic than a thermal reservoir due to the coherence terms (which will be fully discussed in the following sections), using the same equation cannot give us the real temperature which finally should contain the energy of both level distributions and coherency introduced to the reservoir. Eq. (4.1.9) can give us a virtual temperature value, that takes only the level distributions into account without coherency. Then, it is clear that T_{eff} will not be equal to the cavity temperature when a coherent reservoir is injected into the cavity. Even though this seems counter-intuitive, one should always remember that T_{eff} is a fictitious temperature and thermalization is a phenomenon that describes the thermal equilibrium between a reservoir and a system. This issue will be further discussed in following sections as well as next chapter. Additionally, for some *symmetric* multi-level reservoirs, an effective temperature can be defined, as well, which will be demonstrated in the next chapter.

4.1.3 Adiabatic and isochoric processes

In quantum adiabatic process, there is no injection of atomic reservoir into the cavity, so that the mean number of photons produced during the isothermal expansion of a quantum thermodynamic cycle is an invariant. Therefore, we can conclude that there is no exchange between the reservoir and the system just like in a classical adiabatic process. This requires that the probability distribution of energy levels cannot change as well due to Eq. (4.1.5). So this fact makes P_n an invariant of quantum adiabatic process, too. Finally, even though there is no heat intake, work can still be done during this process.

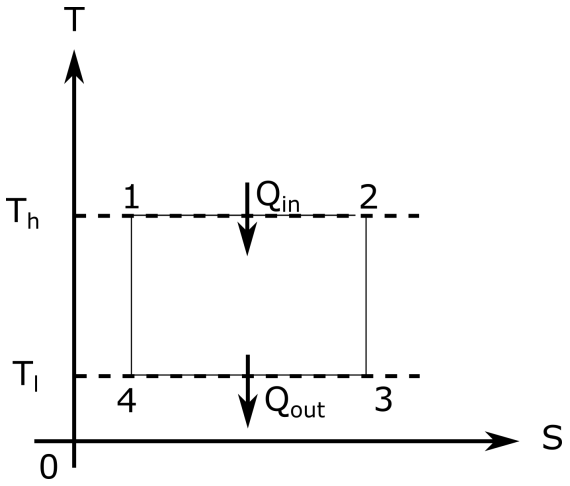

FIGURE 4.2: Temperature-entropy diagram for Carnot engine.

A quantum isochoric process implies a process in which no work can be done just like in its classical analogue. Therefore, due to Eq. (4.1.6) energy eigenvalues, E_n are invariants. However, heat can still be absorbed or released.

There are two important applications of quantum heat engines as Carnot engine and Otto engine. As also known from classical physics, a Carnot engine consists of two isothermal and two adiabatic processes, whereas an Otto engine contains two isochoric and two adiabatic processes. Since we are going to give a brief description of only quantum Carnot engine (QCE), we will skip the details of quantum isochoric processes. A detailed analysis can be obtained via Refs. [38], [13]. An analysis of quantum isobaric processes also exists, [14] as an integral part of quantum Brayton and Diesel cycles, [39].

4.2 Classical Carnot Heat Engine

To generate work out of heat can be done through energy-conversion devices in cycles and such devices are called heat engines, [37]. Heat engines consist of different thermodynamic processes already discussed in the previous section. Carnot heat engine contains two isothermal and two adiabatic or isentropic processes, Fig. 4.2. As perfectly known from thermodynamics, one cannot construct an ideal machine that can fully convert heat energy to work. Work can be totally converted into heat since during this process entropy transfer is zero. However, the inverse is not true, due to the entrance of entropy into the system along with the heat and it does not exit the system with the work. That is why entropy is accumulated throughout the cycle and therefore one should use an entropy sink to get rid of the accumulated entropy during the cycle. So, mathematically

$$Q_H = Q_L + W, \tag{4.2.1}$$

where Q_H is the heat taken, Q_L is the waste heat released out of the system along with the accumulated entropy during the cycle and W is the work. Carnot cycle, being a reversible cycle, puts a higher bound to the engine efficiency. Since Carnot cycle is a reversible cycle, the output entropy is equal to input entropy. Input of the cycle corresponds to the heat intake in the isothermal expansion from $1 \rightarrow 2$ on Fig. 4.2 so that,

$$S_h = \frac{Q_h}{T_h}. \tag{4.2.2}$$

The output of the cycle is the isothermal compression from $3 \rightarrow 4$ on Fig. 4.2,

$$S_l = \frac{Q_l}{T_l}. \tag{4.2.3}$$

Due to the reversibility,

$$S_h = S_l \rightarrow Q_l = \frac{T_l}{T_h} Q_h. \tag{4.2.4}$$

Then substituting Eq. (4.2.4) into Eq. (4.2.1) results in,

$$W = \frac{T_h - T_l}{T_h} Q_h, \tag{4.2.5}$$

so that we define the Carnot efficiency as,

$$\eta_c \equiv \left(\frac{W}{Q_h}\right)_{\text{rev}} = \frac{T_h - T_l}{T_h}. \tag{4.2.6}$$

Carnot efficiency is a higher bound because in fact actual engines consist of irreversible processes and output entropy is always greater than the input entropy. So no actual machine can outperform Carnot engine. One can also calculate how much work can be exactly extracted out of Carnot cycle depended on the type of fuel used via thermodynamic processes, but that is not relevant to our aim here. We showed the Carnot limit classically and now we will review the quantum Carnot engine (QCE) with applications of atomic reservoirs.

4.3 How quantum effects appear in heat engines?

Quantum heat engines are more interesting than classical counterparts, mainly because of the quantum effects appearing in these systems. Here we will first construct a two-level atomic reservoir and then we will work on a three-level atomic reservoir which points to quantum coherence. We are going to investigate the Scully's photo-Carnot engine, [3] from the superoperator approach of master equation analysis and compare it with classical Carnot engine.

4.3.1 Master equation formalism for quantum thermalization problems

The model involves random injections of atoms into the cavity, where atoms are supposed to interact with the cavity once they pass through the cavity, [30, 40]. In each transition, the whole system evolves unitarily in time, which is governed by the interaction Hamiltonian, H_{int} of Tavis-Cummings Model, which has been discussed in Ch. 3.

We assume that j^{th} two-level atom is injected into the cavity at time t_j and passes through the cavity in a time interval of τ. Then the density matrix of the whole system evolves according to, [24, 28]:

$$\begin{aligned} \rho_c(t_j+\tau) &= Tr_A[U(\tau)\rho_A \otimes \rho_c(t_j)U^\dagger(\tau)] \\ &\equiv S(\tau)\rho_c(t_j). \end{aligned} \tag{4.3.1}$$

Here ρ_A is the initial density operator of atomic reservoir sent into the cavity and $S(\tau)$ is the superoperator. A superoperator takes as input a system whose density operator ρ_{ABC} in our case, let it interact with an ancilla of arbitrary size, which is the cavity here ρ_c, perform a unitary operation U on the joint system and finally single out the cavity by tracing out the atomic subsystem, [25].

Atoms will pass through the cavity in a time interval of $(t, t+\delta\tau)$ with a probability of $p\delta\tau$, whereas they will not pass with a probability of $1-p\delta\tau$ since they arrive the cavity randomly. This mechanism of random injections provides a way to model the reservoir, [29, 30]. Here p can be determined by emission rate Γ of atoms. So, when an atom passes through the cavity, the atom and cavity will evolve together, which will be described by the superoperator we introduced. Otherwise, the initial density operator of the cavity will not change, at all.

$$\rho_c(t+\delta t) = p\delta t S(\tau)\rho(t) + (1-p\delta t)\rho(t). \tag{4.3.2}$$

When $\delta t \to 0$, we obtain the master equation which describes the dynamics of our single-mode cavity [11, 12, 41]:

$$\dot{\rho}_c(t) = p\left[S(\tau)-1\right]\rho_c(t). \tag{4.3.3}$$

Eq. (4.3.3) is the most general differential equation regarding the quantum thermal interaction problem discussed in this thesis and it will be widely referred throughout the text.

4.3.2 Thermalization with two-level atomic reservoirs

A schematic for the thermalization of a cavity with two-level reservoirs can be seen in Fig. 4.1. So, here two levels are composed of the states $|e\rangle$ and $|g\rangle$, respectively. Recall that the interaction between a single-mode cavity and a two-level atom is built up through Jaynes-Cummings Model and evolution operator can be found via interaction Hamiltonian. We had already calculated the evolution operator for the Jaynes-Cummings model in Sec. 3.3.1. The most general initial atomic density matrix is,

$$\rho_g = \begin{pmatrix} a_{11} & a_{12} \\ a_{21} & a_{22} \end{pmatrix}. \tag{4.3.4}$$

Inserting the general initial density matrix (5.1.3) into Eq. (5.1.1),

$$S(\tau)\rho(t) = \sum_{i,j=1}^{2} a_{ij} \sum_{n=1}^{2} U_{ni}(\tau)\rho(t)U_{nj}^{\dagger}(\tau) = \rho_c(t_j + \tau). \tag{4.3.5}$$

Then a general master equation follows,

$$\dot{\rho}_c(t) = p \left[\sum_{i,j=1}^{2} a_{ij} \sum_{n=1}^{2} U_{ni}(\tau)\rho(t)U_{nj}^{\dagger}(\tau) - \rho(t) \right]. \tag{4.3.6}$$

Here $n = 1, 2$ corresponds to a basis of $|e\rangle$ and $|g\rangle$, respectively. For convenience, take $\rho = \rho_c$. Let us substitute the elements of approximated version of evolution operator Eq. (3.3.8) into Eq. (5.1.5) to find the master equation for the dynamics of a cavity heated by a two-level atomic reservoir.

$$\begin{aligned} \dot{\rho}(t) \approx (gt)^2 \left(a_{11} \left(a^{\dagger}\rho a - \rho \right) + a_{22} a\rho a^{\dagger} - (a_{11} + a_{22}) \left(\frac{1}{2} a^{\dagger} a\rho + \frac{1}{2} \rho a^{\dagger} a \right) \right) \\ + igt \left(a_{12} \left(\rho a^{\dagger} - a^{\dagger}\rho \right) - a_{21} \left(\rho a - a\rho \right) \right). \end{aligned} \tag{4.3.7}$$

Now we will first show the traditional approach to calculate the equation of motion for mean photon number in the cavity [3] but then due to some problems which will be discussed in a moment we are going to resort to an alternative approach [11]. We can set the vacuum state as the initial state of the cavity field, because we assume that the cavity is not dissipative. Let us calculate the average number of photons existing in the cavity via:

$$\dot{\langle n \rangle} = \sum_{n} n\dot{\rho}_{nn}, \tag{4.3.8}$$

where $\dot{\rho}_{nn}$ can be found via writing Eq. (4.3.7) in Fock number basis, $|n\rangle$ as:

$$\dot{\rho}(t) \approx (gt)^2 \left(a_{11} n\rho_{n-1,n-1} + a_{22} \left((n+1)\rho_{n+1,n+1} - \rho_{n,n} \right) - (a_{11} + a_{22}) n\rho_{n,n} \right). \tag{4.3.9}$$

This is the master equation for diagonal terms in the density matrix of the cavity. Now let us use Eq. (4.3.8):

$$\langle \dot{n} \rangle = (gt)^2 \left(a_{11} \sum_n n^2 \rho_{n-1,n-1} + a_{22} \sum_n n(n+1)\rho_{n+1,n+1} - a_{22} \sum_n n\rho_{n,n} - (a_{11}+a_{22}) \sum_n n^2 \rho_{n,n} \right). \tag{4.3.10}$$

Now we will restate the whole equation with $\rho_{n,n}$, only.

$$\begin{aligned} \langle \dot{n} \rangle &= (gt)^2 \sum_n \left(a_{11}(n+1)^2 + a_{22}(n-1)n - na_{22} - (a_{11}+a_{22})n^2 \right) \rho_{n,n}, \\ &= (gt)^2 \sum_n \left(a_{11}(n+1)^2 + a_{22}(n-1)n - na_{22} - (a_{11}+a_{22})n^2 \right) \rho_{n,n}. \end{aligned} \tag{4.3.11}$$

This leads us,

$$\langle \dot{n} \rangle = (gt)^2 \left(-(a_{22}-a_{11}) \langle n \rangle + a_{11} \right). \tag{4.3.12}$$

Equating Eq. (4.3.12) to zero will give us the mean photon number in the cavity when the system is thermalized.

$$\langle n \rangle_{\text{ss}} = \frac{a_{11}}{a_{22}-a_{11}}. \tag{4.3.13}$$

Even though the first method gives us a mean photon number value, it does not provide us an interval of validity. For example, can we take $a_{11} > a_{22}$? Such a choice will present negative values for the mean number of photons, which does not make sense. That is why we are going to introduce the second method. Let us first state,

$$\langle \hat{n}(t_j + \tau) \rangle = \text{Tr} \left[\rho(t_j + \tau) \right]. \tag{4.3.14}$$

and note the relations with using the cyclic property of trace,

$$\begin{aligned} \text{Tr} \left[a\rho a^\dagger a^\dagger a \right] &= \left\langle n^2 \right\rangle - \langle n \rangle, \\ \text{Tr} \left[a^\dagger \rho a a^\dagger a \right] &= 1 + 2\langle n \rangle + \left\langle n^2 \right\rangle, \\ \text{Tr} \left[\rho a^\dagger a \right] &= \langle n \rangle, \\ \text{Tr} \left[a^\dagger a \rho a^\dagger a \right] &= \text{Tr} \left[\rho a^\dagger a a^\dagger a \right] = \left\langle n^2 \right\rangle. \end{aligned} \tag{4.3.15}$$

Now we can calculate the mean photon number.

$$\begin{aligned} \langle \hat{n}(t_j + \tau) \rangle = &\left[1 + 2(gt)^2 (a_{11} - a_{88}) \right] \langle \hat{n}(t_j) \rangle \\ &+ 2(gt)^2 a_{11}, \end{aligned} \tag{4.3.16}$$

The increment of average photon number between two passings will be,

$$\Delta \langle \hat{n}(t_j + \tau) \rangle = \left[1 + 2(gt)^2(a_{11} - a_{88})\right] \langle \hat{n}(t_j) \rangle . \tag{4.3.17}$$

Then the increment ratio,

$$k = \frac{\Delta \langle \hat{n}(t_j + \tau) \rangle}{\Delta \langle \hat{n}(t_j) \rangle} = 1 + 2(gt)^2(a_{11} - a_{88}). \tag{4.3.18}$$

Since we assumed the initial state is vacuum state, the average number of photons after the first passing will be,

$$\langle \hat{n}(\tau) \rangle = (gt)^2 (2a_{11}) . \tag{4.3.19}$$

By using Eqns. (4.3.18) and (4.3.19) one can state the average photon number in the cavity field after j^{th} passing,

$$\langle \hat{n}(t_j) \rangle = \sum_{i=1}^{j} k^{i-1} \langle \hat{n}(\tau) \rangle . \tag{4.3.20}$$

For average photon number is being convergent, $k \leq 1$ should be satisfied in Eq. (4.3.20). This leads us,

$$1 + 2(gt)^2(a_{11} - a_{88}) < 1, \tag{4.3.21}$$

which requires,

$$a_{11} < a_{88}. \tag{4.3.22}$$

It can be verified that Eq. (4.3.20) gives us the Eq. (4.3.13) in addition to an expected condition of $a_{88} > a_{11}$. This condition in fact makes sure that the mean photon number cannot be negative or infinite. It also says that the population at the ground level of the atom should be greater than the population at the excited level to have a finite and positive mean photon number in the cavity. This is our first encounter with the first condition of quantum thermal interaction. We are going to demonstrate that this condition is in fact universal for the quantum thermal interaction realized in micromaser model, [16–18] in the next chapter. As a final note, for a two-level atomic reservoir the coherence terms in the master Eq. (4.3.7) are in fact single-photon processes and even though they seem to be useless for the mean photon number in the cavity, they contribute the mean photon number [12] as a cavity drive. However, we are not going to analyze single and two-photon processes in this thesis.

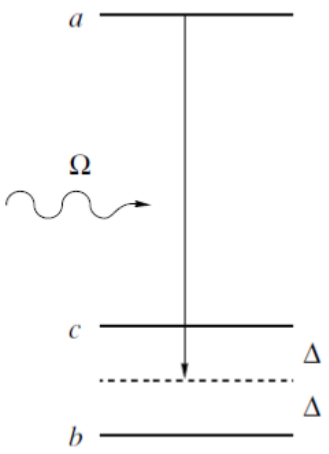

FIGURE 4.3: Energy level structure of phaseonium atomic reservoir or fuel.

4.3.3 Thermalization with degenerate two-level atomic reservoir - phaseonium fuel

It is possible to modify a two-level atom a bit to create degeneracy in the ground energy level so that we can inject some coherency that can be useful in the thermalization and hence work output of the cavity. See Fig. 4.3 for a three-level atom with a degeneracy at the ground level. This atomic reservoir has been first developed by Scully et al. [3] and named as *phaseonium fuel* due to its characteristic of quantum coherency which will be explained shortly. Quan et al. [41] approached to the derivation of master equation of this problem from the superoperator method that we have utilized in this thesis, contrary to the microscopic method of Rostovtsev et al. in [42]. For this, they first state the ground level with its degeneracy:

$$|G\rangle = \frac{|g_1\rangle + |g_2\rangle}{\sqrt{2}}, \tag{4.3.23}$$

in the Jaynes-Cummings interaction Hamiltonian of

$$H_{\text{int}} = \hbar g \, |e\rangle \langle G| \, a + \text{h.c.}, \tag{4.3.24}$$

where a is the annihilation operator and g is the coupling constant between the three level atom and cavity. We will write the evolution operator of this interaction Hamiltonian,

$$U_n(t) = \exp(-iH_{\text{int}}t) = \begin{pmatrix} \cos(gt\sqrt{n}) & \frac{-i}{\sqrt{2}}\sin(gt\sqrt{n}) & \frac{-i}{\sqrt{2}}\sin(gt\sqrt{n}) \\ \frac{-i}{\sqrt{2}}\sin(gt\sqrt{n}) & \cos^2\left(\frac{gt}{2}\sqrt{n}\right) & -\sin^2\left(\frac{gt}{2}\sqrt{n}\right) \\ \frac{-i}{\sqrt{2}}\sin(gt\sqrt{n}) & -\sin^2\left(\frac{gt}{2}\sqrt{n}\right) & \cos^2\left(\frac{gt}{2}\sqrt{n}\right) \end{pmatrix}, \tag{4.3.25}$$

for a cavity with n excitations. Also note that the atomic reservoir will be of the following form,

$$\rho = \begin{pmatrix} a_{11} & 0 & 0 \\ 0 & a_{22} & a_{23} \\ 0 & a_{32} & a_{33} \end{pmatrix}. \tag{4.3.26}$$

It is possible to use atomic reservoir density matrix Eq. (4.3.26) and the evolution operator Eq. (4.3.25) in a general form of master equation similar to Eq. (5.1.5), however there is an easier approach to derive the master equation. That is substituting $a_{22} + a_{33} + 2|a_{23}|\cos\phi$ instead of a_{22} in master Eqs. (4.3.7) and (4.3.9) for two-level atomic reservoir, [43]. In short,

$$\begin{aligned}\dot{\rho}(t) \approx (gt)^2 \left(a_{11} n \rho_{n-1,n-1} + (a_{22} + a_{33} + 2|a_{23}|\cos\phi)\left((n+1)\rho_{n+1,n+1} - \rho_{n,n}\right)\right) \\ - (gt)^2 \left((a_{11} + a_{22} + a_{33} + 2|a_{23}|\cos\phi) n \rho_{n,n}\right).\end{aligned} \tag{4.3.27}$$

Then, similarly the equation of motion for the mean photon number is,

$$\langle \dot{n} \rangle = (gt)^2 \left(-2(a_{22} + a_{33} + 2|a_{23}|\cos\phi - a_{11})\langle n \rangle + 2a_{11}\right), \tag{4.3.28}$$

and the steady state solution for the mean photon number is,

$$\langle n \rangle_{\text{ss}} = \frac{a_{11}}{a_{22} + a_{33} + 2|a_{23}|\cos\phi - a_{11}}, \tag{4.3.29}$$

with the condition of $a_{22} + a_{33} + 2|a_{23}|\cos\phi > a_{11}$. One can clearly see that by tuning phase angle ϕ between two degenerate ground levels in our atomic reservoir, we can change the mean number of photons existing in the cavity after thermalization. In fact, it is clear that when $\phi = \pi$ which corresponds to maximum coherency, the mean photon number will be maximum. Through Eq. (4.1.7), an increase in mean photon number means an increase in the work capability of the cavity. Let us now see the details of this work capability in a bit more detail.

4.3.4 Photo-Carnot engine with phaseonium fuel

Photo-Carnot cycle consists of two isothermal and two adiabatic processes. In the calculation of the work out of a quantum Carnot cycle, we are going to follow Refs. [3, 41]. See the temperature-entropy diagram for QCE in Fig. 4.4, which points to an extra area of extracted work with the usage of phaseonium fuel. Eq. (4.3.14) can be written in a

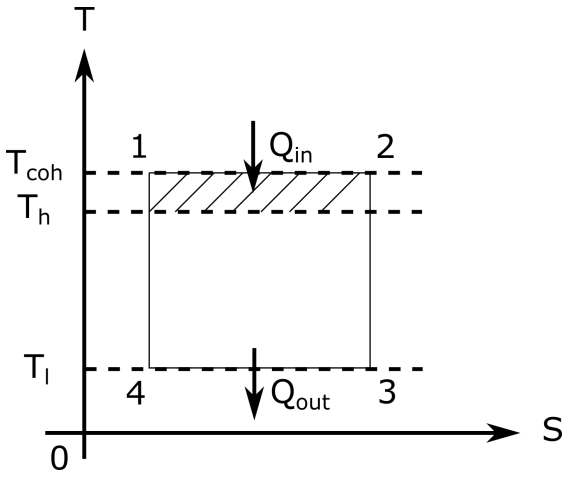

FIGURE 4.4: Temperature-entropy diagram for quantum Carnot engine (QCE).

neater way:

$$\langle n\rangle_{\text{ss,coh}} = \langle n\rangle_{\text{ss}} (1 - \langle n\rangle_{\text{ss}} \epsilon \cos\phi) = \frac{kT_{\text{eff}}}{\hbar\omega}(1 - \langle n\rangle_{\text{ss}} \epsilon \cos\phi), \tag{4.3.30}$$

where $\langle n\rangle_{\text{ss}}$ is the mean photon number of two-level atoms without coherency and $\epsilon = 2|a_{23}|/(a_{22} + a_{33})$. Note that the temperature definition can be done via,

$$\langle n\rangle_{\text{ss}} = \frac{kT_{\text{eff}}}{\hbar\omega}, \tag{4.3.31}$$

because of the high temperature limit instead of (Bose-) Einstein distribution. Similarly since we can write,

$$\langle n\rangle_{\text{ss,coh}} = \frac{kT_{\text{coh}}}{\hbar\omega}. \tag{4.3.32}$$

Then, the relation between effective temperature of two-level reservoirs and coherent reservoirs is,

$$T_{\text{coh}} = T_{\text{eff}}(1 - \langle n\rangle_{\text{ss}} \epsilon \cos\phi). \tag{4.3.33}$$

Quantum isothermal expansion implies a heat intake and quantum isothermal compression, an entropy sink. Therefore via Fig. 4.4,

$$\begin{aligned} Q_{\text{in}} &= T_{\text{coh}} \left[S_{\text{coh}}(2) - S_{\text{coh}}(1)\right] \\ Q_{\text{out}} &= T_{\text{l}} \left[S_{\text{l}}(3) - S_{\text{l}}(4)\right]. \end{aligned} \tag{4.3.34}$$

On the other hand, quantum adiabatic process implicates that the mean photon number cannot change throughout the process.

$$\begin{aligned} \langle n_{\text{coh}}(2)\rangle &= \langle n_{\text{l}}(3)\rangle \\ \langle n_{\text{coh}}(4)\rangle &= \langle n_{\text{l}}(1)\rangle. \end{aligned} \tag{4.3.35}$$

Again due to the high temperature limit,

$$\frac{\hbar\omega(1)}{kT_{\text{coh}}} = \frac{\hbar\omega(4)}{kT_{\text{l}}}, \qquad \frac{\hbar\omega(2)}{kT_{\text{coh}}} = \frac{\hbar\omega(3)}{kT_{\text{l}}}. \tag{4.3.36}$$

Additionally, we assume the frequency change is quasistatic because of the adiabatic change during this process, which leads us

$$\omega(1) = \omega(2), \qquad \omega(3) = \omega(4). \tag{4.3.37}$$

Using the entropy expression

$$S_i = k\ln(\langle n^i \rangle + 1) + \frac{\hbar\omega_i \langle n^i \rangle}{T^i}, \tag{4.3.38}$$

we can conclude that $S_{\text{coh}}(2) - S_{\text{coh}}(1) = S_{\text{l}}(3) - S_{\text{l}}(4)$. Then let us take the ratio of $Q_{\text{out}}/Q_{\text{in}}$:

$$\frac{Q_{\text{out}}}{Q_{\text{in}}} = \frac{T_{\text{l}}}{T_{\text{coh}}}. \tag{4.3.39}$$

Since the efficiency is defined as,

$$\eta_{\text{coh}} = \frac{W}{Q_{\text{in}}} = \frac{Q_{\text{in}} - Q_{\text{out}}}{Q_{\text{in}}} = 1 - \frac{T_{\text{l}}}{T_{\text{coh}}}. \tag{4.3.40}$$

Now substitute Eq. (4.3.33) into Eq. (4.3.40),

$$\eta_{\text{coh}} = 1 - \frac{T_{\text{l}}}{T_{\text{eff}}(1 - \langle n \rangle_{\text{ss}} \epsilon \cos\phi)}. \tag{4.3.41}$$

Since we work in high temperature limit, Scully in [3] argues that $a_{22} \approx a_{33} \approx 1/3$, which states $\epsilon = 3|a_{23}|$. Now let us modify Eq. (4.3.41) according to this approximation,

$$\eta_{\text{coh}} = 1 - \frac{T_{\text{l}}}{T_{\text{eff}}(1 - 3\langle n \rangle_{\text{ss}} |a_{23}| \cos\phi)}. \tag{4.3.42}$$

The Carnot efficiency is $\eta = 1 - \frac{T_{\text{l}}}{T_{\text{eff}}}$. If we arrange Eq. (4.3.42), we can end up with

$$\eta_{\text{coh}} = \eta - \frac{T_{\text{l}}}{T_{\text{eff}}} \left(\frac{3\langle n \rangle_{\text{ss}} |a_{23}| \cos\phi)}{1 - 3\langle n \rangle_{\text{ss}} |a_{23}| \cos\phi)} \right). \tag{4.3.43}$$

If we assume $3\langle n \rangle_{\text{ss}} |a_{23}| \cos\phi) \ll 1$,

$$\eta_{\text{coh}} = \eta - \frac{T_{\text{l}}}{T_{\text{eff}}} 3\langle n \rangle_{\text{ss}} |a_{23}| \cos\phi). \tag{4.3.44}$$

When the coherence phase is chosen maximally as $\phi = \pi$, coherent efficiency beats Carnot efficiency. This is one of the most important peculiarity that quantum mechanics introduces to thermodynamics. As a second peculiarity, see that when $\phi = \pi$ and

$T_{\text{eff}} = T_1$ are chosen,

$$\eta_{\text{coh}} = 3 \langle n \rangle_{\text{ss}} |a_{23}|, \tag{4.3.45}$$

so that quantum Carnot engine extracts work from a single reservoir. Finally before ending this section, let us note that quantum thermodynamics does not violate any fundamental law of physics with these observations. In fact, the energy that makes this outperforming possible comes from coherency added to the system. Zubairy discussed this point clearly and showed that adding coherency to the system in fact excesses the extra work done in QCE, [15]. Ref. [42] also extensively discusses how to prepare the coherent atomic reservoirs. To sum up, the injection of coherent atomic reservoirs transports an extra energy into the cavity from outside in order to extract more work than classically possible.

Up to here, we have demonstrated the importance of isothermal processes or specifically the thermalization of cavity with the atomic reservoirs. Calculating a mean number of photons has utmost importance in order to extract a useful work output. Now, finally we will work out the thermalization process of two-level atomic pairs (TLAPs) [11] as a preliminary to next chapters.

4.4 Thermalization with two-level atomic pairs

Let us first write down a specially chosen density matrix of atomic reservoir,

$$\rho = \begin{pmatrix} a_{11} & 0 & 0 & 0 \\ 0 & a_{22} & a_{23} & 0 \\ 0 & a_{32} & a_{33} & 0 \\ 0 & 0 & 0 & a_{44} \end{pmatrix}. \tag{4.4.1}$$

Note that this state is a mixed state and it is in fact,

$$\rho = a_{11} |ee\rangle \langle ee| + (\sqrt{a_{22}} |eg\rangle + \sqrt{a_{33}} |ge\rangle) (\sqrt{a_{22}} \langle eg| + \sqrt{a_{33}} \langle ge|) + a_{44} |gg\rangle \langle gg|. \tag{4.4.2}$$

Some terms are chosen zero on purpose, in order to get rid of single- and two-photon processes. As will be seen after analysis, the coherence terms a_{23} and a_{32} are important. However the contribution of these coherence terms will be different from the ones we observed in three-level atoms in previous section. Recall that the general form of master equation is Eq. (5.1.2) and the approximated evolution operator for 2-atom reservoir is Eq. (3.3.21). Let us substitute both the density matrix Eq. (4.4.1) and evolution

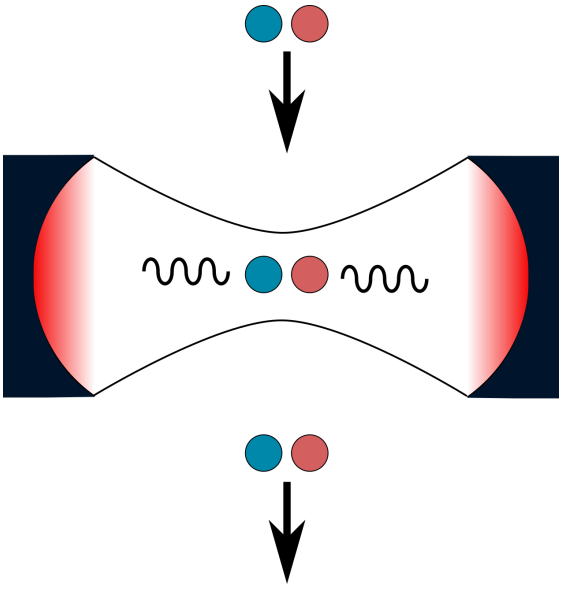

FIGURE 4.5: Model schematic of the a quantum thermal interaction between a cavity and two-atom reservoir.

operator into the general master equation and obtain,

$$\dot{\rho} \approx p(gt)^2 \left(a_{11}(2a^\dagger \rho a - \rho a^\dagger a - a^\dagger a \rho - 2\rho) + a_{44}(2a\rho a^\dagger - \rho a^\dagger a - a^\dagger a \rho)\right) \\ - (a_{22} + a_{33}) \left(2\rho a^\dagger a - a\rho a^\dagger - a^\dagger \rho a + \rho\right) + (a_{23} + a_{32}) \left(a\rho a^\dagger + a^\dagger \rho a - a^\dagger a \rho - \rho a^\dagger a - \rho\right). \tag{4.4.3}$$

By following the same steps of first or (preferably) second method in Sec. 4.3.2, one can obtain the equation of motion for the mean photon number,

$$\langle n \rangle_{\text{ss}} = \frac{2a_{11} + a_{22} + a_{33} + a_{23} + a_{32}}{2(a_{44} - a_{11})}, \tag{4.4.4}$$

with the condition of $a_{44} > a_{11}$. This condition once more emphasizes the fact that the population at the ground energy level should be greater than the population at the excited energy level. The details of this behaviour will be discussed in the next chapter as a peculiarity of quantum thermal interaction. Additionally Eq. (4.4.4) shows the effect of the coherence terms at the nominator of the mean photon number, contrary to the three-level atomic reservoir. The efficiency of coherent reservoirs will also be a topic of next chapter.

Chapter 5

Thermalization with 3-atom reservoirs

We had calculated the evolution operator for the interaction of a single mode cavity and three atoms in Chapter 3 and then we introduced the formalism for the quantum master equation governing the quantum heat engine and thermalization model in Chapter 4. First of all, we are going to derive the quantum master equation for the thermalization of a cavity with three atoms in this chapter. In Secs. 5.1.1 and 5.1.3 we presented the results for W and GHZ states, respectively and compared them. In Sec. 5.1.2, we discussed a special reservoir that cannot thermalize a cavity, which is a non-classical and unexpected behaviour for an intuitive thermal interaction. In Sec. 5.1.4, we analyzed specific mixed state reservoirs to explicitly backup the rules of optimum thermalization we proposed at the end of section.

5.1 General form of quantum master equation with 3-atom reservoirs

Let us restate the most general form of quantum master equation of the QHE model,

$$\hat{\rho}_c(t+\delta t) = p\delta t S(\tau)\hat{\rho}(t) + (1-p\delta t)\hat{\rho}(t). \tag{5.1.1}$$

$$\dot{\hat{\rho}}_c(t) = p\left[S(\tau)-1\right]\hat{\rho}_c(t). \tag{5.1.2}$$

The most general initial TLAT (two level atomic triplets) density matrix is,

$$\hat{\rho}_g = \begin{pmatrix} a_{11} & a_{12} & a_{13} & a_{14} & a_{15} & a_{16} & a_{17} & a_{18} \\ a_{21} & a_{22} & a_{23} & a_{24} & a_{25} & a_{26} & a_{27} & a_{28} \\ a_{31} & a_{32} & a_{33} & a_{34} & a_{35} & a_{36} & a_{37} & a_{38} \\ a_{41} & a_{42} & a_{43} & a_{44} & a_{45} & a_{46} & a_{47} & a_{48} \\ a_{51} & a_{52} & a_{53} & a_{54} & a_{55} & a_{56} & a_{57} & a_{58} \\ a_{61} & a_{62} & a_{63} & a_{64} & a_{65} & a_{66} & a_{67} & a_{68} \\ a_{71} & a_{72} & a_{73} & a_{74} & a_{75} & a_{76} & a_{77} & a_{78} \\ a_{81} & a_{82} & a_{83} & a_{84} & a_{85} & a_{86} & a_{87} & a_{88} \end{pmatrix}. \tag{5.1.3}$$

Inserting the general initial density matrix (5.1.3) into Eq. (5.1.1),

$$S(\tau)\hat{\rho}(t) = \sum_{i,j=1}^{8} a_{ij} \sum_{n=1}^{8} \hat{U}_{mi}(\tau)\hat{\rho}(t)\hat{U}^{\dagger}_{mj}(\tau) = \hat{\rho}_c(t_j + \tau). \tag{5.1.4}$$

Then a general master equation follows,

$$\dot{\hat{\rho}}_c(t) = p \left[\sum_{i,j=1}^{8} a_{ij} \sum_{n=1}^{8} \hat{U}_{mi}(\tau)\hat{\rho}(t)\hat{U}^{\dagger}_{mj}(\tau) - \hat{\rho}(t) \right]. \tag{5.1.5}$$

In next section, we are going to state the conditions for thermalization to occur in a cavity when the cavity interacts with 3-atom reservoirs. These conditions are reached with a thermodynamic analysis of some 3-atom reservoirs, e.g. W and GHZ states as well some mixed states. We are going to show that thermalization is possible with perfect and imperfect W states in the first section and thermalization is not possible with a perfect GHZ state in the second section. We will also show some specific pure state cannot thermalize a cavity ever. Finally we will present optimized and mixed 3-atom reservoirs. Motivated by the whole analysis, we are going to summary the conditions of thermalization we observe in a system of a cavity and a 3-atom reservoir.

5.1.1 Thermalization with W States

We will set our initial density matrix for the atoms as W state: $W = (|001\rangle + |010\rangle + |100\rangle)/\sqrt{3}$. W state is an multipartite entangled quantum state. Then the initial density operator

is,

$$\rho_g = \begin{pmatrix} 0 & 0 & 0 & 0 & 0 & 0 & 0 & 0 \\ 0 & 0 & 0 & 0 & 0 & 0 & 0 & 0 \\ 0 & 0 & 0 & 0 & 0 & 0 & 0 & 0 \\ 0 & 0 & 0 & a_{44} & 0 & a_{46} & a_{47} & 0 \\ 0 & 0 & 0 & 0 & 0 & 0 & 0 & 0 \\ 0 & 0 & 0 & a_{64} & 0 & a_{66} & a_{67} & 0 \\ 0 & 0 & 0 & a_{74} & 0 & a_{76} & a_{77} & 0 \\ 0 & 0 & 0 & 0 & 0 & 0 & 0 & 0 \end{pmatrix}, \tag{5.1.6}$$

where $a_{ij} = 1/3$ for $i, j = 4, 6, 7$. As expected, $\sum_{i=1}^{8} a_{ii} = 1$. Inserting W state into Eq. (5.1.4),

$$\begin{aligned} \rho(t_j + \tau) \approx\ & (g\tau)^2 (a_{44} + a_{66} + a_{77}) \left(2a\rho_c a^\dagger + a^\dagger \rho_c a - \rho - \frac{3}{2} a^\dagger a \rho_c - \frac{3}{2} \rho_c a^\dagger a \right) \\ & + p(g\tau)^2 (a_{46} + a_{64} + a_{47} + a_{74} + a_{67} + a_{76}) \left(a\rho_c a^\dagger + a^\dagger \rho_c a - \rho_c a^\dagger a - a^\dagger a \rho_c - \rho \right) \\ & + \rho(t). \end{aligned} \tag{5.1.7}$$

Then, the master equation for the cavity evolution heated by 3-atom reservoir is:

$$\begin{aligned} \dot{\rho} \approx\ & p(g\tau)^2 (a_{44} + a_{66} + a_{77}) \left(2a\rho_c a^\dagger + a^\dagger \rho_c a - \rho - \frac{3}{2} a^\dagger a \rho_c - \frac{3}{2} \rho_c a^\dagger a \right) \\ & + p(g\tau)^2 (a_{46} + a_{64} + a_{47} + a_{74} + a_{67} + a_{76}) \left(a\rho_c a^\dagger + a^\dagger \rho_c a - \rho_c a^\dagger a - a^\dagger a \rho_c - \rho \right). \end{aligned} \tag{5.1.8}$$

Following Ref. [11] we can set the vacuum state as the initial state of the cavity field, because we assume that the cavity is not dissipative. Also we can state that a cavity heated by a W reservoir will always be in thermal state, since Eq. (5.1.8) does not have any off-diagonal terms, hence there will be no population in the off-diagonal terms. Let us now calculate the average number of photons existing in the cavity.

$$\langle \dot{n} \rangle = \sum_n n \dot{\rho}_{nn}, \tag{5.1.9}$$

where $\dot{\rho}_{nn}$ can be found via writing Eq. (5.1.8) in Fock number basis, $|n\rangle$ as:

$$\begin{aligned} \dot{\rho}_{nn} =\ & p(g\tau)^2 (a_{44} + a_{66} + a_{77}) \left(2(n+1)\rho_{n+1,n+1} + n\rho_{n-1,n-1} - (1+3n)\rho_{n,n} \right) \\ & + p(g\tau)^2 (a_{46} + a_{64} + a_{47} + a_{74} + a_{67} + a_{76}) \left((n+1)\rho_{n+1,n+1} + n\rho_{n-1,n-1} - (1+2n)\rho_{n,n} \right). \end{aligned} \tag{5.1.10}$$

For convenience let us introduce new variables as $D = (a_{44} + a_{66} + a_{77})$ and $C = (a_{46} + a_{64} + a_{47} + a_{74} + a_{67} + a_{76})$ where D stands for 'diagonal' and C stands for 'coherent'.

$$\begin{aligned}\langle \dot{n} \rangle = p(g\tau)^2 D \left(\sum_n 2n(n+1)\rho_{n+1,n+1} + \sum_n n^2 \rho_{n-1,n-1} - \sum_n n\rho_{n,n} - 3\sum_n n^2 \rho_{n,n} \right) \\ + p(g\tau)^2 C \left(\sum_n n(n+1)\rho_{n+1,n+1} + \sum_n n^2 \rho_{n-1,n-1} - 1\sum_n n\rho_{n,n} - 2\sum_n n^2 \rho_{n,n} \right).\end{aligned} \tag{5.1.11}$$

Now we will restate the whole equation with $\rho_{n,n}$, only.

$$\begin{aligned}\langle \dot{n} \rangle = p(g\tau)^2 D \sum_n \left(2(n-1)n + (n+1)^2 - n - 3n^2 \right) \rho_{n,n} \\ + p(g\tau)^2 C \sum_n \left((n-1)n + (n+1)^2 - n - 2n^2 \right) \rho_{n,n}.\end{aligned} \tag{5.1.12}$$

This leads us,

$$\langle \dot{n} \rangle = -D \langle n \rangle + C + D. \tag{5.1.13}$$

Equating Eq. (5.1.13) to 0 will give us the mean photon number in the cavity when the system is thermalized.

$$\langle n \rangle_{\text{ss}} = \frac{C+D}{D} = 1 + \frac{a_{46} + a_{64} + a_{47} + a_{74} + a_{67} + a_{76}}{a_{44} + a_{66} + a_{77}}. \tag{5.1.14}$$

Since the summation of elements at diagonal is 1, it can be observed that adding coherence terms will boost up the mean photon number in the cavity.

$$\langle n \rangle_{\text{ss}} = 1 + a_{46} + a_{64} + a_{47} + a_{74} + a_{67} + a_{76}. \tag{5.1.15}$$

Therefore, in the case of using a W state, the mean number of photons in the cavity will increase from 0 to 3, which implies a thermalization of the cavity with entangled atoms. Let us also note that the initial photon number in the cavity does not affect the final number of photons after thermalization. Therefore, if we start with, say 5 photons in the cavity, we will cool the cavity with a W state to 3 photons.

An intuitive picture may give us a deeper insight about this process. A W state consists of an unequal distribution of ground and excited levels with ground levels being occupied more than excited levels. Such a state will be energizing the cavity as well as de-energizing it. In fact, the excited levels in the reservoir imply a gain whereas the ground levels point to a loss of the cavity. Although we did not explicitly introduce the loss to the system, the cavity leaks its energy through the interaction of atoms indirectly, which might seen from the Lindblad form of master Eq. (5.1.8). An example of this

interpretation can be seen through the driving of cavity with $|ggg\rangle$ atoms, only. Such a state will always cool the cavity to zero photon because $|ggg\rangle$ itself does not contain any energy to feed the cavity, so that it brings the cavity to its own temperature as a reservoir.

It is tempting to physically understand why cavity thermalization with W type of 3-atom fuel gives a mean photon number of three. Even though this question is not straightforward to answer, we argue that each of three atoms emit a photon simultaneously acting together via cavity field and coherence terms. We draw attention to the observation that the emission and absorption rates get equal when three photons exist in the cavity, so that the thermalization is achieved. This interpretation implies the existence of an energy balance between the coherent reservoir and cavity after many cycles of reservoir injections. In fact, exactly this observation makes us think that the cavity and the coherent reservoir form a monolithic system all together, whose energy exchange does not affect the balance which must be a condition for thermalization. In order to show this point more clearly, let us first repeat this Gedanken experiment with only one state: $|egg\rangle$, which is simpler due to the lack of superposition and hence coherency. After many cycles of state $|egg\rangle$, we expect that the cavity will have an energy of only one photon due to the lack of coherence terms and in fact this is exactly the amount of energy in the atomic reservoir. Similarly, one can have two photons activating the aforementioned mechanism when the partially coherent state $\frac{1}{2}\left(|egg\rangle + |geg\rangle\right)$ is sent into cavity, again due to the coherence terms $a_{46} = a_{64} = 1/2$ and rate equalization of TLATs when cavity field is populated with two photons. To sum up, thermalization, by definition, represents a thermal equilibrium state where the emission and absorption rates of atomic reservoir become equal so that energy exchange between reservoir and cavity does not affect the equilibrium state. Even though this is hard to see with coherent reservoirs, due to symmetric energy distribution of W state, it may be possible to see the thermalization of a cavity with a W state through the interpretation presented above. Finally, adding coherence to the atomic reservoir is shown to increase the mean photon number in the cavity.

W state is a symmetric state, therefore provides us a way to calculate the effective temperature even though it is a multi-level reservoir. Each of the three atoms has a probability set of $P_e = 1/3$ and $P_g = 2/3$, which gives us an opportunity to write the effective temperature as,

$$T_{\text{eff}} = \frac{1}{k_B \beta_{\text{eff}}} = \frac{\hbar\omega}{k_B}\left(\ln\frac{P_g}{P_e}\right)^{-1} = \frac{\omega}{k_B}\ln 2. \tag{5.1.16}$$

This result can be verified through the temperature calculation of photon field in the cavity after thermalization via,

$$T_{\text{coh}} = \frac{1}{k_B \beta_{\text{coh}}} = \frac{\hbar\omega}{k_B} \left(\ln \left(\frac{1 + \langle n \rangle_{\text{ss}}}{\langle n \rangle_{\text{ss}}} \right) \right)^{-1}. \tag{5.1.17}$$

If we substitute Eq. (5.1.15) into Eq. (5.1.17), we obtain

$$T_{\text{coh}} = \frac{\hbar\omega}{k_B} \left(\ln \left(\frac{2 + 2\left(\text{Re}[a_{46}] + \text{Re}[a_{67}] + \text{Re}[a_{47}]\right)}{1 + 2\left(\text{Re}[a_{46}] + \text{Re}[a_{67}] + \text{Re}[a_{47}]\right)} \right) \right)^{-1}, \tag{5.1.18}$$

which is the temperature of the cavity after thermalization has been established. As seen from Eq. (5.1.18), when there is no coherence term, $T_{\text{coh}} = T_{\text{eff}}$, [4]. However, one should note that T_{eff} is only a virtual temperature where the coherency of W type reservoir is not taken into account. Therefore, the temperature of the cavity after thermalization should be regarded as the temperature at the thermal equilibrium. Finally, when probabilities of W state are substituted, calculation leads us to $T = 3.47\omega\hbar/k$.

Now we are going to introduce a general set of parameters for W state, which preserves both normalizability and trace preservation, to see how the mean number of photons change when the probabilities of W state change.

$$\begin{aligned} |W\rangle = \cos\theta \cos\frac{\psi}{2} |egg\rangle + \sin\theta \cos\frac{\psi}{2} \mathrm{e}^{i\phi} |geg\rangle \\ + \sin\frac{\psi}{2} \mathrm{e}^{i\delta} |gge\rangle \,. \end{aligned} \tag{5.1.19}$$

Then the mean photon number in terms of general parameters is,

$$\langle n \rangle_{\text{ss}} = 1 + \sin 2\theta \cos^2\frac{\psi}{2} \cos\phi + \cos\theta \sin\psi \cos\delta + \sin\theta \sin\psi \cos(\phi - \delta). \tag{5.1.20}$$

When $\delta = 0, \phi = 0$ are chosen, the mean number of photons vary with respect to θ and ψ as in Fig. 5.1. Here, the maximum number corresponds to a W state configuration. Therefore, we can conclude that the most entangled state gives the most optimum solution among the W type of states.

5.1.2 A 3-atom reservoir which can never thermalize

Let us look at a state configuration of,

$$|\mathrm{E}\rangle = \frac{1}{\sqrt{3}} \left(|eeg\rangle + |ege\rangle + |gee\rangle \right). \tag{5.1.21}$$

Such a state has an unequal distribution of populations at excited and ground levels of atoms and the population at the excited levels are in majority, which indicates a

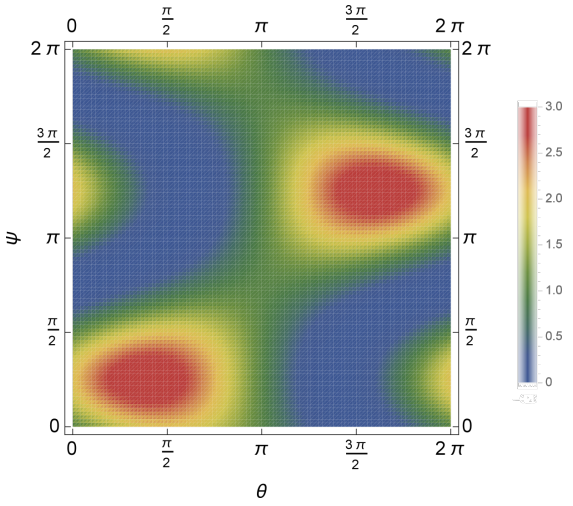

FIGURE 5.1: (Color online) The mean number of photons with respect to the general parameters θ and ψ, when $\delta = 0$ and $\phi = 0$.

considerable amount of heating up in the cavity. As an example of quantum thermal interaction, we would expect a thermal equilibrium at the end with a great amount of photons. However, we will see that thermal equilibrium is not the case here. Inserting E state into Eq. (5.1.4) leads us to

$$\begin{aligned}\rho(t_j+\tau) \approx{}& (g\tau)^2\left(a_{22}+a_{33}+a_{55}\right)\left(a\rho_c a^\dagger + 2a^\dagger\rho_c a - 2\rho - \frac{3}{2}a^\dagger a\rho_c - \frac{3}{2}\rho_c a^\dagger a\right)\\ &+ (g\tau)^2\left(a_{23}+a_{25}+a_{32}+a_{35}+a_{52}+a_{53}\right)\left(a\rho_c a^\dagger + a^\dagger\rho_c a - \rho_c a^\dagger a - a^\dagger a\rho_c - \rho\right)\\ &+ \rho(t_j).\end{aligned} \tag{5.1.22}$$

Then the master equation is derived as,

$$\begin{aligned}\dot{\rho} \approx{}& p(g\tau)^2\left(a_{22}+a_{33}+a_{55}\right)\left(a\rho_c a^\dagger + 2a^\dagger\rho_c a - 2\rho - \frac{3}{2}a^\dagger a\rho_c - \frac{3}{2}\rho_c a^\dagger a\right)\\ &+ p(g\tau)^2\left(a_{23}+a_{25}+a_{32}+a_{35}+a_{52}+a_{53}\right)\left(a\rho_c a^\dagger + a^\dagger\rho_c a - \rho_c a^\dagger a - a^\dagger a\rho_c - \rho\right).\end{aligned} \tag{5.1.23}$$

Instead of using Eq. (5.1.9) to find the equation of motion for the mean number of photons in the cavity, we are going to utilize another approach which analytically forbids the existence of a steady-state solution. For this, we first state the following,

$$\langle\hat{n}(t_j+\tau)\rangle = \mathrm{Tr}\left[\rho(t_j+\tau)\right]. \tag{5.1.24}$$

and note the relations with using the cyclic property of trace,

$$\begin{aligned}
\mathrm{Tr}\left[a\rho a^\dagger a^\dagger a\right] &= n^2 - n, \\
\mathrm{Tr}\left[a^\dagger \rho a a^\dagger a\right] &= 1 + 2n + n^2, \\
\mathrm{Tr}\left[\rho a^\dagger a\right] &= n, \\
\mathrm{Tr}\left[a^\dagger a\rho a^\dagger a\right] &= \mathrm{Tr}\left[\rho a^\dagger a a^\dagger a\right] = n^2,
\end{aligned} \tag{5.1.25}$$

we can calculate the mean photon number.

$$\langle \hat{n}(t_j + \tau)\rangle = \left[1 + (g\tau)^2 \sum_i a_{ii}\right] \langle \hat{n}(t_j)\rangle + (g\tau)^2 \left(2\sum_i a_{ii} + \sum_{ij, i\neq j} a_{ij}\right), \tag{5.1.26}$$

for $i, j = 2, 3, 5$. The increment of average photon number between two passings will be,

$$\Delta \langle \hat{n}(t_j + \tau)\rangle = \left[1 + (g\tau)^2 \sum_i a_{ii}\right] \langle \hat{n}(t_j)\rangle . \tag{5.1.27}$$

Then the increment ratio,

$$k = \frac{\Delta \langle \hat{n}(t_j + \tau)\rangle}{\Delta \langle \hat{n}(t_j)\rangle} = 1 + (g\tau)^2 \sum_i a_{ii}. \tag{5.1.28}$$

Since we assumed the initial state is vacuum state, the average number of photons after the first passing will be,

$$\langle \hat{n}(\tau)\rangle = (g\tau)^2 \left(2\sum_i a_{ii} + \sum_{ij, i\neq j} a_{ij}\right). \tag{5.1.29}$$

By using Eqns. (5.1.28) and (5.1.29) one can state the average photon number in the cavity field after j^{th} passing,

$$\langle \hat{n}(t_j)\rangle = \sum_{i=1}^{j} k^{i-1} \langle \hat{n}(\tau)\rangle . \tag{5.1.30}$$

For average photon number is being convergent, $k \leq 1$ should be satisfied in Eq. (5.1.30). This leads us,

$$1 + (g\tau)^2 \sum_i a_{ii} \leq 1, \tag{5.1.31}$$

which requires,

$$\sum_i a_{ii} \leq 0. \tag{5.1.32}$$

When we think of a density matrix, this condition cannot be satisfied due to the trace preservation. Then, $\langle \hat{n}(t_j) \rangle$ is divergent all the time, which shows there cannot be thermalization with the state $|\mathrm{E}\rangle$ regardless of the probabilities. Therefore, the state $|\mathrm{E}\rangle$ lases with exponentially increasing photon number in the cavity. Lack of a mean value for the photon number also disregards a definition for temperature. In the end what we could say is that $|\mathrm{E}\rangle$ reservoir and cavity cannot be in thermal equilibrium. Physically this can be interpreted as that the emission and absorption rates of reservoirs will never be equal to each other at any Fock state of the cavity field throughout the process. And reason for the unbalanced rates is related to the population ratio of excited to ground energy levels. Accumulation of atoms with an energy more than a critical value drives the cavity to lase.

5.1.3 Thermalization with GHZ States

Another well-known 3 atom state is GHZ state: $\left(|000\rangle + |111\rangle\right)/\sqrt{2}$.

$$\rho_{\mathrm{GHZ}} = \begin{pmatrix} a_{11} & 0 & 0 & 0 & 0 & 0 & 0 & a_{18} \\ 0 & 0 & 0 & 0 & 0 & 0 & 0 & 0 \\ 0 & 0 & 0 & 0 & 0 & 0 & 0 & 0 \\ 0 & 0 & 0 & 0 & 0 & 0 & 0 & 0 \\ 0 & 0 & 0 & 0 & 0 & 0 & 0 & 0 \\ 0 & 0 & 0 & 0 & 0 & 0 & 0 & 0 \\ 0 & 0 & 0 & 0 & 0 & 0 & 0 & 0 \\ a_{81} & 0 & 0 & 0 & 0 & 0 & 0 & a_{88} \end{pmatrix}, \tag{5.1.33}$$

where $a_{ij} = 1/2$ for $i, j = 1, 8$ and $\sum_{i=1}^{8} a_{ii} = 1$. Similar to the analysis of W state, we will insert GHZ state, Eq. (5.1.33) into the general master equation, Eq. (5.1.4) to obtain a specific master equation:

$$\dot{\rho}(t) \approx p(g\tau)^2 \left(3a_{11} a^\dagger \rho a + 3a_{88} a \rho a^\dagger - \frac{3}{2}(a_{11} + a_{88}) \left(\rho a^\dagger a + a^\dagger a \rho \right) - 3a_{11}\rho \right). \tag{5.1.34}$$

The terms a_{18} and a_{81} are neglected, since their lowest order appearing in the equation is $(g\tau)^3$. Let us calculate the mean photon number with first rewriting the master equation for diagonal terms ρ_{nn},

$$\dot{\rho}_{nn} = p(g\tau)^2 \left(3a_{11} n \rho_{n-1,n-1} + 3a_{88}(n+1)\rho_{n+1,n+1} - \frac{3}{2}(a_{11} + a_{88}) 2n \rho_{nn} - 3a_{11}\rho_{nn} \right). \tag{5.1.35}$$

By utilizing Eq. (5.1.9), one can find the equation of motion for the mean photon number in the cavity contact with GHZ reservoir.

$$\langle \dot{n} \rangle = \sum_n n\dot{\rho}_{nn} = p(g\tau)^2 3(a_{11} - a_{88}) \langle n \rangle + 3a_{11}. \tag{5.1.36}$$

Eq. (5.1.36) leads us to a mean photon number of:

$$\langle n \rangle_{\text{ss}} = \frac{a_{11}}{a_{88} - a_{11}}, \tag{5.1.37}$$

where $a_{88} > a_{11}$ for Eq. (5.1.37). This condition can be derived with utilizing the method in previous section 5.1.2. Since $a_{11} = a_{88} = 1/2$ in a perfect GHZ state, Eq. (5.1.37) will be useless to calculate the mean photon number in a cavity fed with GHZ states. Otherwise, Eq. (5.1.37) results of an infinity as the mean photon number for a GHZ reservoir, which points to lasing in fact. One can see that the equation of motion for the mean number of photon in the case of a GHZ reservoir is

$$\langle \dot{n} \rangle = p(g\tau)^2 \frac{3}{2}. \tag{5.1.38}$$

Therefore, we can conclude that the mean number of photon increases linearly with time and never stabilizes around an equilibrium. This observation implies the lack of steady-state solution for GHZ state, hence no thermalization can be established for the cavity and GHZ type of reservoir. It is important to realize that GHZ state has an equal distribution of population at excited and ground levels of reservoir atoms. Since the existence of thermalization requires an equilibrium between emission and absorption rates of atoms and these rates change according to the photon population in the cavity, we can conclude that emission and absorption rates will never be equal to each other at any time of the process for a cavity heated by GHZ state. On top of that, we can also conclude that emission rate will always exceed the absorption rate due to the lack of thermalization observed. To conclude, cavity with GHZ state will lase.

Additionally, one can see that lack of thermalization exists when the superposition of only one atom is used as reservoir, $(|g\rangle + |e\rangle)/\sqrt{2}$, [43] as well as two atoms, $(|gg\rangle + |ee\rangle)/\sqrt{2}$, [11]. One might realize a similarity between lasing of GHZ state and lasing without population inversion (LWI), [19] where even a small population at the excited level can drive the system to lasing due to the coherence between two degenerate ground levels. In LWI, emission rate of atoms beat the absorption rate simply because absorption rate becomes zero. However, in lasing with GHZ states there is population inversion, hence absorption rate of GHZ atoms is not zero. The lasing mechanism of GHZ states is different and one may realize that for LWI solution of Eq. (5.1.36) will result of an exponentially

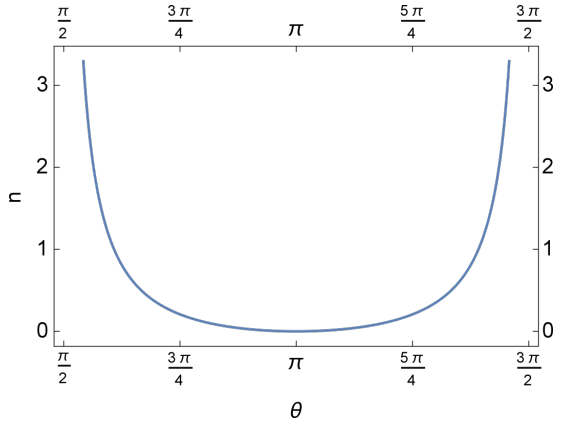

FIGURE 5.2: (Color online) The mean number of photons with respect to the general parameter θ.

increasing function, whereas for GHZ states, the solution leads us to a linearly increasing function. Both lack of a thermal equilibrium, though the reasons why they lase are distinct. LWI is a demonstration of pure quantum effects appearing due to the superposition of wavefunctions, [16], however under instantaneous limit the coherent terms of GHZ state are neglected and lasing is due to the population at the excited level and the fact that absorption rate cannot exceed the emission rate.

A general set of parameters for GHZ state follows,

$$|\mathrm{GHZ}\rangle = \cos\frac{\theta}{2}\,|eee\rangle + \sin\frac{\theta}{2}\mathrm{e}^{i\phi}\,|ggg\rangle\,. \tag{5.1.39}$$

Then the mean photon number in terms of general parameters is,

$$\langle n\rangle_{\mathrm{ss}} = \frac{\cos^2\frac{\theta}{2}}{\sin^2\frac{\theta}{2} - \cos^2\frac{\theta}{2}}. \tag{5.1.40}$$

As can be seen from the Eq. (5.1.40), the steady-state solution of the mean number of photons in the cavity does not depend on the coherence, angle ϕ between the states. Analytically this happens because of the instantaneous limit we applied at the start, so that we neglected effect of the coherence terms in the master equation. However a careful look might give a deeper insight. One should note that the coherence terms of GHZ state contain three photon processes since they in fact connect two farthest states, $|eee\rangle$ and $|ggg\rangle$ through the cavity. Therefore, the time interval, δt of TLATs passing through the cavity will not be enough to excite these processes, which is also reasonable when we think of the weak coupling constant between TLATs and cavity. As a result due to the deficiency in setting up the indirect coupling between $|eee\rangle$ and $|ggg\rangle$, a cavity heated by GHZ state will not enjoy the effect of coherence terms.

Slightly tweaking the probabilities of GHZ state will open a way to thermalization. Note

that $a_{88} > a_{11}$, which gives a greater weight to the state $|ggg\rangle$, so that a new steady-state forms for the system to reside. Fig. ?? which sketches the mean number of photon with respect to θ, demonstrates the thermalization with imperfect GHZ states when θ is chosen sufficiently close to $\pi/2$ but not $\pi/2$. One can maybe achieve the thermalization with a photon number as much as possible at such a configuration, however with a cost of stabilization. The change in the mean photon number will be dramatic closer to the singularity, $\theta = \pi/2$ even with a little fluctuation at θ parameter, which will alter the thermalized environment of cavity continuously. As a conclusion choosing a θ value closer to singularity but not at singularity points out to an *apparent efficiency* in thermalization due to the unstable nature of cavity dynamics around singularity. So, it does not offer practical use. The so-called stable thermalization with GHZ states seems possible only around $\theta = \pi$, which leads us to a mean photon number under one. In this sense, W state is a better reservoir than GHZ state with offering the full use of its coherence terms in the thermalization.

5.1.4 Mixed and optimized 3-atom reservoirs

Final issue that we would like to address is the optimization after thermalization has been achieved. It is possible to make up 3 atom reservoirs with mixed states which might give more optimum results than W state.

Let us start with the following mixed state,

$$\rho_{\mathrm{AS1,m}} = \frac{1}{3}\left(|egg\rangle\langle eeg| + |geg\rangle\langle geg| + 2\,|egg\rangle\langle geg|\right) + \frac{1}{3}|eeg\rangle\langle eeg|\,. \tag{5.1.41}$$

Writing down its master equation,

$$\begin{aligned}\dot{\rho} \approx\ & p(g\tau)^2\,(a_{44}+a_{66})\left(2a\rho_c a^\dagger + a^\dagger\rho_c a - \rho - \frac{3}{2}a^\dagger a\rho_c - \frac{3}{2}\rho_c a^\dagger a\right)\\ &+ p(g\tau)^2\,(a_{46}+a_{64})\left(a\rho_c a^\dagger + a^\dagger\rho_c a - \rho_c a^\dagger a - a^\dagger a\rho_c - \rho\right)\\ &+ p(g\tau)^2 a_{22}\left(a\rho_c a^\dagger + 2a^\dagger\rho_c a - 2\rho - \frac{3}{2}a^\dagger a\rho_c - \frac{3}{2}\rho_c a^\dagger a\right)\end{aligned} \tag{5.1.42}$$

The differential equation for mean number of photons as,

$$\langle\dot{n}\rangle = p(g\tau)^2\,(a_{22} - (a_{44}+a_{66}))\,\langle n\rangle + 2a_{22} + a_{44} + a_{66} + 2\mathrm{Re}[a_{46}]. \tag{5.1.43}$$

Then the steady-state solution is,

$$\langle n\rangle_{\mathrm{ss}} = \frac{2a_{22} + a_{44} + a_{66} + 2\mathrm{Re}[a_{46}]}{a_{44} + a_{66} - a_{22}}, \tag{5.1.44}$$

where the condition $a_{44} + a_{66} > a_{22}$ shows up when the approach in Sec. 5.1.2 is followed. Substituting the probabilities of $\rho_{\mathrm{AS1,m}}$ into Eq. (5.1.44) gives 6 as mean photon number. One should note that the mixed state $\rho_{\mathrm{AS1,m}}$ is in fact a combination of $|gge\rangle$, $|geg\rangle$ and $|eeg\rangle$ with coherent terms between $|gge\rangle$ and $|geg\rangle$ but without any coherent term regarding $|eeg\rangle$. Because latter shows up in master equation with one photon processes weighted with $g\tau$ as emission-absorption rate, so that they might be affecting the cavity dynamics. Therefore, one should make a deeper analysis to determine the effects of such single or multi photon processes on cavity dynamics before elaborating on aforementioned pure states. Additionally, note that the state $\rho_{\mathrm{AS1,m}}$ consists of maximally energetic basis vectors which can also be thermalized. Therefore, it is reasonable to expect that $\rho_{\mathrm{AS1,m}}$ outperforms W state.

Let us take a minimally energetic mixed state,

$$\rho_{\mathrm{AS2,m}} = \frac{1}{2}\left(|ggg\rangle\langle ggg| + |egg\rangle\langle egg|\right), \tag{5.1.45}$$

Steady state solution for the photon number can be similarly computed as,

$$\langle n\rangle_{\mathrm{ss}} = \frac{a_{44}}{a_{44} + 3a_{88}}. \tag{5.1.46}$$

Calculation shows that it should thermalize at a photon number of $1/4$, which is pretty low when compared to even mixed GHZ states. The final example is,

$$\rho_{\mathrm{AS3,m}} = \frac{1}{3}\left(|ggg\rangle\langle ggg| + |eee\rangle\langle eee| + |egg\rangle\langle egg|\right). \tag{5.1.47}$$

Notice that both the states $\rho_{\mathrm{AS3,m}}$ and $\rho_{\mathrm{AS1,m}}$ have maximum excited levels, whereas the state $\rho_{\mathrm{AS1,m}}$ has coherence terms appearing in the equation for the mean number of photons, so that the state $\rho_{\mathrm{AS1,m}}$ produces 6 photons. However, the equation for mean photon number of $\rho_{\mathrm{AS3,m}}$ is,

$$\langle n\rangle_{\mathrm{ss}} = \frac{3a_{11} + a_{44}}{a_{44} + 3a_{88} - 3a_{11}}, \tag{5.1.48}$$

where the condition $a_{44} + 3a_{88} > 3a_{11}$ shows up when the approach in Sec. 5.1.2 is followed. Eq. (5.1.48) gives us a mean photon number of 4. Therefore, it is obvious that the reservoir that contains coherence outperforms the reservoir without any coherence.

We can now state some rules for optimum thermalization of a single mode cavity.
1. Condition of critical energy: In order to compensate the inequality between absorption and emission rates of TLATs, the populations at the ground levels should be strictly greater than the populations at excited levels for a TLAT. This will establish the thermal equilibrium for a quantum thermal interaction in micromaser theory.

2. Condition of optimum thermalization: After the thermal equilibrium has been established, we should try to maximize the populations at excited levels in TLATs, because exactly these energetic populations heat up the cavity to a mean photon number which can be used for a temperature definition.
3. Condition of quantum coherency: Coherent states boost up the temperature of the cavity when compared to thermal states.

Chapter 6

Conclusions

Improving an intuitive understanding for the thermalization of a cavity via atomic reservoirs might open a new door to utilize quantum thermodynamic systems more efficiently as quantum heat engines and refrigerators. For this purpose, we developed an analytical tool for 3-atom reservoirs which interact with a cavity instantaneously through Tavis-Cummings Model. The results for the interaction of 1-atom reservoirs and cavity, [3, 12] are well-known. Additionally, thermalization effects of some special 2-atom reservoirs have been recently studied [11]. The observations we made for all 1-3 atom reservoirs can be summarized concisely and might be generalized to all multi-atom reservoirs, which nevertheless requires further research.

For thermalization to occur, detailed balance between emission and absorption rates of TLATs, or in general atomic reservoirs, should be established at a cavity temperature via the number of photons existing in cavity. Otherwise the cavity lases instead of being thermalized as in the case of GHZ and AS1 states. In fact it is not a coincidence that these specific states do contain more populations at excited energy levels than at ground levels or exactly equal numbers of populations at excited and ground levels. In short, due to these energetic TLATs cavity does not stabilize around a well-defined temperature. This important observation lets us state the first rule regarding the reservoir for the thermalization of a cavity: *A good reservoir should contain more population at its ground energy levels than excited energy levels for thermal equilibrium to be realized.* W state is an example of such reservoirs which rearranges the cavity temperature as the cavity will contain three photons.

By following the first rule, it is possible to thermalize even a lasing cavity when the probabilities of TLATs are modified in the favour of ground energy levels. Nevertheless W state is a better reservoir than GHZ state due to both the contribution of W state's coherence terms and lack of stable thermalization for GHZ type reservoirs. The condition

of critical energy also verifies the observation that $|\mathrm{AS1}\rangle$ type of reservoir in Sec. 5.1.2 cannot thermalize a cavity, at all.

We observe that some mixed states can outperform the efficiency of W state. First point to note is that these mixed states are designed in a way that they do not contain any coherence terms which might trigger one or two photon processes. Our observations intuitively point to a condition in reservoir design for optimized cavities: *After letting the population at the ground energy levels beat the population at the excited energy levels, one should maximize the population at the excited energy levels*, since exactly these energetic energy levels feed the cavity. Final observation about mixed states also reveals a second condition for optimization: *Cavities are heated up more when coherence terms are utilized.*

Another conclusion we would like to state is that the most entangled W state gives the most optimum mean photon number among all W-type reservoirs. This observation emphasizes the importance of entanglement in extracting work out of a cavity thermalized with W-type reservoirs.

To conclude, a further work might include both analytical and numerical study on the effects of single- and two-photon processes on thermalization. Finally, an integral part of future study should contain a generalization of our results to multi-atom reservoirs, which might exploit the presented analytical machinery of evolution operator calculations, Ch. 3.

Bibliography

[1] L. D. Landau and E. M. Lifshitz. *Statistical Physics, Vol. 5 of Course of Theoretical Physics*. Pegamon Press LTD., London, 1958.

[2] F. Reif. *Statistical Physics*. McGraw-Hill, Inc., Massachusetts, 1965.

[3] Marlan O. Scully, M. Suhail Zubairy, Girish S. Agarwal, and Herbert Walther. Extracting work from a single heat bath via vanishing quantum coherence. *Science*, 299(5608):862–864, 2003. doi: 10.1126/science.1078955. URL http://www.sciencemag.org/content/299/5608/862.abstract.

[4] H. T. Quan, Yu-xi Liu, C. P. Sun, and Franco Nori. Quantum thermodynamic cycles and quantum heat engines. *Phys. Rev. E*, 76:031105, Sep 2007. doi: 10.1103/PhysRevE.76.031105. URL http://link.aps.org/doi/10.1103/PhysRevE.76.031105.

[5] Noah Linden, Sandu Popescu, and Paul Skrzypczyk. How small can thermal machines be? the smallest possible refrigerator. *Phys. Rev. Lett.*, 105:130401, Sep 2010. doi: 10.1103/PhysRevLett.105.130401. URL http://0-link.aps.org.divit.library.itu.edu.tr/doi/10.1103/PhysRevLett.105.130401.

[6] Amikam Levy and Ronnie Kosloff. Quantum absorption refrigerator. *Phys. Rev. Lett.*, 108:070604, Feb 2012. doi: 10.1103/PhysRevLett.108.070604. URL http://0-link.aps.org.divit.library.itu.edu.tr/doi/10.1103/PhysRevLett.108.070604.

[7] Leonard J. Schulman and Umesh V. Vazirani. Molecular scale heat engines and scalable quantum computation. In *Proceedings of the Thirty-first Annual ACM Symposium on Theory of Computing*, STOC '99, pages 322–329, New York, NY, USA, 1999. ACM. ISBN 1-58113-067-8. doi: 10.1145/301250.301332. URL http://0-doi.acm.org.divit.library.itu.edu.tr/10.1145/301250.301332.

[8] P. O. Boykin, Tal Mor, Vwani Roychowdhury, Farrokh Vatan, and Rutger Vrijen. Algorithmic cooling and scalable nmr quantum computers. *Proceedings of the*

National Academy of Sciences of the United States of America, 99(6):3388–3393, 2002.

[9] Tomáš Man al, Tae-Kyu Ahn, Gregory S. Engel, Robert E. Blankenship, Graham R. Fleming, Yuan-Chung Cheng, Elizabeth L. Read, and Tessa R. Calhoun. Evidence for wavelike energy transfer through quantum coherence in photosynthetic systems. *Nature*, 446(7137):782–786, 2007.

[10] Ferdi Altintas, Ali Ü. C. Hardal, and Özgür E. Müstecaplıoğlu. Rabi model as a quantum coherent heat engine: From quantum biology to superconducting circuits. *Phys. Rev. A*, 91:023816, Feb 2015. doi: 10.1103/PhysRevA.91.023816. URL http://link.aps.org/doi/10.1103/PhysRevA.91.023816.

[11] Hai Li, Jian Zou, Wen-Li Yu, Bao-Ming Xu, Jun-Gang Li, and Bin Shao. Quantum coherence rather than quantum correlations reflect the effects of a reservoir on a system's work capability. *Phys. Rev. E*, 89:052132, May 2014. doi: 10.1103/PhysRevE.89.052132. URL http://link.aps.org/doi/10.1103/PhysRevE.89.052132.

[12] Jie-Qiao Liao, H. Dong, and C. P. Sun. Single-particle machine for quantum thermalization. *Phys. Rev. A*, 81:052121, May 2010. doi: 10.1103/PhysRevA.81.052121. URL http://link.aps.org/doi/10.1103/PhysRevA.81.052121.

[13] Y. V. Rostovtsev, A. B. Matsko, N. Nayak, M. S. Zubairy, and M. O. Scully. Improving engine efficiency by extracting laser energy from hot exhaust gas. *Phys. Rev. A*, 67:053811, May 2003. doi: 10.1103/PhysRevA.67.053811. URL http://link.aps.org/doi/10.1103/PhysRevA.67.053811.

[14] H. T. Quan. Quantum thermodynamic cycles and quantum heat engines. ii. *Physical Review E - Statistical, Nonlinear, and Soft Matter Physics*, 79(4):041129, 2009.

[15] M. S. Zubairy. The Photo-Carnot Cycle: The Preparation Energy for Atomic Coherence. In D. P. Sheehan, editor, *Quantum Limits to the Second Law*, volume 643 of *American Institute of Physics Conference Series*, pages 92–97, November 2002. doi: 10.1063/1.1523787.

[16] Marlan O. Scully and M. Suhail Zubairy. *Quantum Optics*. Cambridge University Press, Cambridge, 2001.

[17] Marlan O. Scully and Willis E. Lamb. Quantum theory of an optical maser. i. general theory. *Phys. Rev.*, 159:208–226, Jul 1967. doi: 10.1103/PhysRev.159.208. URL http://link.aps.org/doi/10.1103/PhysRev.159.208.

[18] Marlan O. Scully and Willis E. Lamb. Quantum theory of an optical maser. ii. spectral profile. *Phys. Rev.*, 166:246–249, Feb 1968. doi: 10.1103/PhysRev.166.246. URL http://link.aps.org/doi/10.1103/PhysRev.166.246.

[19] Marlan O. Scully, Shi-Yao Zhu, and Athanasios Gavrielides. Degenerate quantum-beat laser: Lasing without inversion and inversion without lasing. *Phys. Rev. Lett.*, 62:2813–2816, Jun 1989. doi: 10.1103/PhysRevLett.62.2813. URL http://link.aps.org/doi/10.1103/PhysRevLett.62.2813.

[20] Daniel M Greenberger, Michael A Horne, and Anton Zeilinger. Going beyond bell's theorem. In *Bell's theorem, quantum theory and conceptions of the universe*, pages 69–72. Springer, 1989.

[21] W. Dür, G. Vidal, and J. I. Cirac. Three qubits can be entangled in two inequivalent ways. *Phys. Rev. A*, 62:062314, Nov 2000. doi: 10.1103/PhysRevA.62.062314. URL http://0-link.aps.org.divit.library.itu.edu.tr/doi/10.1103/PhysRevA.62.062314.

[22] Kazuyuki Fujii, Kyoko Higashida, Ryosuke Kato, Tatsuo Suzuki, and Yukako Wada. Explicit form of the evolution operator of tavis-cummings model : Three and four atoms cases. *Int.J.Geom.Meth.Mod.Phys.*, 1:721–730, 2004. doi: arXiv:quant-ph/0409068.

[23] C. W. Gardiner. *Handbook of Stochastic Methods*. Springer, Heidelberg, 1985.

[24] C. W. Gardiner. *Quantum Noise, a handbook of markovian and non-markovian quantum stochastic methods with applications to quantum optics*. Springer, Heidelberg, 2000.

[25] Phillip Kaye, Raymond Laflamme, and Michele Mosca. *An Introduction to Quantum Computing*. Oxford Univ. Press, Oxford, 2007.

[26] W.H. Louisell. *Quantum statistical properties of radiation*. Wiley, New York, 1973.

[27] Reinhard Mahnke, Jevgenijs Kaupužs, and Ihor Lubashevsky. *Physics of stochastic processes. How randomness acts in time.* Weinheim: Wiley-VCH, 2009. doi: 10.1002/9783527626090.

[28] Gernot Schaller. *Open Quantum Systems Far from Equilibrium*. Springer, Switzerland, 2014.

[29] J. V. Neumann. Physical applications of the ergodic hypothesis. *Proceedings of the National Academy of Sciences of the United States of America*, 18(3):263–266, 1932.

[30] J. D. Cresser. Quantum-field model of the injected atomic beam in the micromaser. *Phys. Rev. A*, 46:5913–5931, Nov 1992. doi: 10.1103/PhysRevA.46.5913. URL http://link.aps.org/doi/10.1103/PhysRevA.46.5913.

[31] Ceren B. Dag. *A Readout Method for a Flux Qubit-Resonator System in the Ultrastrong Coupling Regime*. BSc. thesis for Istanbul Technical University Faculty of Electrical and Electronics Engineering, 2015.

[32] E. T. Jaynes and F. W. Cummings. Comparison of quantum and semiclassical radiation theories with application to the beam maser. *Proc. IEEE*, 51, 1963.

[33] Michael Tavis and Frederick W. Cummings. Exact solution for an n-molecule¯radiation-field hamiltonian. *Phys. Rev.*, 170:379–384, Jun 1968. doi: 10.1103/PhysRev.170.379. URL http://link.aps.org/doi/10.1103/PhysRev.170.379.

[34] Barry M. Garraway. The Dicke model in quantum optics: Dicke model revisited. *Physical and Engineering Sciences*, 369(1939):1137–1155, 2011. doi: 10.1098/rsta.2010.0333. URL http://dx.doi.org/10.1098/rsta.2010.0333.

[35] H. E. D. Scovil and E. O. Schulz-DuBois. Three-level masers as heat engines. *Phys. Rev. Lett.*, 2:262, Mar 1959.

[36] Deniz Turkpence and Ozgur E. Mustecaplioglu. Quantum fuel with multilevel atomic coherence for ultrahigh specific work in a photonic carnot engine. *Pre-print*, 2014. arXiv:1503.01627.

[37] Charles Kittel and Herbert Kroemer. *Thermal Physics*. W. H. Freeman and Company, 1980.

[38] Kieu, T. D. Quantum heat engines, the second law and maxwell's daemon. *Eur. Phys. J. D*, 39(1):115–128, 2006. doi: 10.1140/epjd/e2006-00075-5. URL http://dx.doi.org/10.1140/epjd/e2006-00075-5.

[39] Herbert B. Callen. *Thermodynamics*. John Wiley & Sons, Inc., New York, N.Y., 1960.

[40] D. Meschede, H. Walther, and G. Müller. One-atom maser. *Phys. Rev. Lett.*, 54: 551–554, Feb 1985. doi: 10.1103/PhysRevLett.54.551. URL http://link.aps.org/doi/10.1103/PhysRevLett.54.551.

[41] H. T. Quan, P. Zhang, and C. P. Sun. Quantum-classical transition of photon-carnot engine induced by quantum decoherence. *Phys. Rev. E*, 73:036122, Mar 2006. doi: 10.1103/PhysRevE.73.036122. URL http://link.aps.org/doi/10.1103/PhysRevE.73.036122.

[42] Yu. V. Rostovtsev, Z. E. Sariyianni, and M. O. Scully. Extracting energy from a single heat bath via vanishing quantum coherence: Iii. master equation derivation. *Laser Physics Nonlinear and Quantum Optics*, 13:375–385, 2003.

[43] M. O. Scully. Extracting Work from A Single Heat Bath via Vanishing Quantum Coherence II: Microscopic Model. 643:83–91, November 2002. doi: 10.1063/1.1523786.